www.directivepublications.org

The Journal of Clinical Medicine

ISSN 2995-6315

Research Article

Longitudinal Multiomics Analysis Of Cerebrospinal Fluid Identifies Amyloid- And Tau-Independent Pathways Associated With Cognitive Impairment.

Joby Jose[1,2], Natalie Astraea[3], Xiaomeng Wu[2,3], Ryan Butler[4], Austin Quach[5], Olivia Choi[5], Serly Khosravian[6], Anne Nolty[6], Robert A Kloner[7], Alfred N Fonteh[1*], Anju Vasudevan[2*ϕ],

[1]Biomarkers and Neurodisease Mechanism Laboratory, Department of Neurosciences, Huntington Medical Research Institutes (HMRI), Pasadena, California, USA.

[2]Angiogenesis and Brain Development Laboratory, Department of Neurosciences, Huntington Medical Research Institutes (HMRI), Pasadena, California, USA.

[3]Analytical Biochemistry Core Laboratory, Huntington Medical Research Institutes (HMRI), Pasadena, California, USA.

[4]Clinical Neurosciences, Huntington Medical Research Institutes (HMRI), Pasadena, California, USA.

[5]Dalton Bioanalytics Inc., California NanoSystems Institute, Los Angeles, California, USA.

[6]Fuller Theological Seminary, Pasadena, California, USA.

[7]Cardiovascular Laboratory, Huntington Medical Research Institutes (HMRI), Pasadena, California, USA.

Abstract

Background/Objectives: Cerebrospinal fluid (CSF) amyloid and tau, plasma p-tau217, brain magnetic resonance (MR) imaging, positron emission tomography (PET) imaging, and neuropsychological assessments are routinely employed in Alzheimer's disease (AD) diagnosis. However, beyond amyloid and tau, the longitudinal dynamics of other CSF analytes remain unexplored. To explore this gap, we conducted an exploratory multiomics analysis of CSF samples collected from cognitively unimpaired (CU) individuals and reassessed the same participants after their transition to cognitively impaired (CI).

Method: Adults over 60 years of age were classified as cognitively unimpaired (CU) or cognitively impaired (CI) based on a neuropsychological battery. Multiomics using multidimensional liquid chromatography and ultrasensitive mass spectrometry of CSF was conducted at the CU state and reassessed after participants transitioned to the CI state.

Results: The mean interval for conversion from CU to CI was 4.6 ± 3.5 years. We identified 1,478 CSF analytes, comprising 4 electrolytes, 202 metabolites, 343 lipids, and 929 proteins. These findings should be interpreted as discovery-based observations requiring validation in larger cohorts. Potassium, 5 metabolites, and 33 lipids were significantly altered in the CI state relative to the CU state. Among CSF proteins, 29 were downregulated, and 41 were upregulated with cognitive impairment. Differentially expressed proteins, including those associated with the extracellular matrix, exosomes, transport vesicles, and the plasma membrane, were enriched predominantly in membrane-associated fractions. Pathway analysis revealed that cognitive impairment was associated with alterations in amyloid fibril formation, intercellular communication, signaling, stress responses, cell death, and protein refolding.

Conclusions: These exploratory findings suggest that cognitive decline may be accompanied by complex molecular alterations and identify candidate pathways that warrant validation in larger longitudinal studies.

Keywords: Cognition, Cerebrospinal fluid (CSF), Multiomics analysis, Longitudinal study, altered metabolism, Dysfunctional protein processing, Immune dysregulation, Changes in cell adhesion, Altered energy pathways.

*** Co-senior author and ϕ Corresponding Author: Anju Vasudevan.** Angiogenesis and Brain Development Laboratory, Department of Neurosciences, Huntington Medical Research Institutes (HMRI), Pasadena, California, USA. **Email:** Anju.Vasudevan@hmri.org.

Received: 03-August-2026, Manuscript No. TJOCM - 6062 **; Editor Assigned:** 05-August-2026 **; Reviewed:** 01-September-2026, QC No. TJOCM - 6062 **; Published:** 25-September-2026, **DOI:** 10.52338/tjocm.2026.6062.

Citation: Anju Vasudevan. Longitudinal Multiomics Analysis Of Cerebrospinal Fluid Identifies Amyloid- And Tau-Independent Pathways Associated With Cognitive Impairment. The Journal of Clinical Medicine. 2026 September; 19(1). doi: 10.52338/tjocm.2026.6062.

Copyright © 2026 Anju Vasudevan. This is an open access article distributed under the Creative Commons Attribution License, which permits unrestricted use, distribution, and reproduction in any medium, provided the original work is properly cited.

INTRODUCTION

Dementia encompasses a heterogeneous group of neurodegenerative disorders characterized by the progressive deterioration of cognitive function. Among these diseases, Alzheimer's disease (AD) is the most prevalent and devastating, accounting for most dementia cases worldwide. Clinically, AD is characterized by a gradual decline in memory and executive function, ultimately leading to loss of independence and the inability to perform daily activities. Neuropathologically, AD is defined by widespread neurodegeneration, with hallmark features, including extracellular amyloid-β (Aβ) deposition, intraneuronal tau pathology, synaptic dysfunction, and progressive neuronal loss, all of which contribute to the trajectory of cognitive decline [1-4].

At the molecular level, AD is driven by the accumulation of Aβ plaques and neurofibrillary tangles (NFTs), which disrupt neuronal function and impair cognition [5]. The transmembrane amyloid precursor protein (APP) can be processed via nonamyloidogenic or amyloidogenic pathways, the latter giving rise to Aβ42 peptides that aggregate to form plaques [6,7]. In parallel, the microtubule-associated protein tau (MAPT) undergoes hyperphosphorylation and misfolding, leading to the loss of microtubule stabilization and axonal dysfunction [8,9].

Aging remains the strongest risk factor for AD, yet the rate and severity of cognitive decline vary considerably across individuals, indicating the contribution of additional pathogenic mechanisms. Increasing evidence implicates mitochondrial dysfunction and reactive oxygen species (ROS) production as critical drivers of disease initiation and progression [10]. Aβ aggregates disrupt mitochondrial morphology, reduce ATP production, impair respiratory capacity, and promote oxidative stress. Sustained oxidative stress, in turn, enhances tau hyperphosphorylation and microtubule destabilization, thereby accelerating NFT pathology [10].

In addition to amyloid and tau, AD is associated with diverse molecular alterations, including neuroinflammation, synaptic dysfunction, oxidative stress, impaired glucose metabolism, cholinergic deficits, and vascular injury [11-13]. These multifactorial changes underscore the complexity of AD biology and highlight the need for broader mechanistic insights to inform the discovery of candidate biomarkers and pathways for future investigation. Collectively, these highlight the limitations of current diagnostic and therapeutic strategies that focus primarily on amyloid and tau. Despite decades of research, therapies directly targeting these pathologies have yielded only modest clinical benefits, underscoring the critical need to identify additional biological pathways that contribute to disease onset and progression.

Multiomics approaches provide a powerful exploration strategy for addressing this challenge by integrating information across multiple molecular layers, including genes, transcripts, proteins, metabolites, and lipids. This system-level perspective enables the identification of novel biomarkers for early diagnosis and prognosis, as well as mechanistic insights into dysregulated pathways that may yield new therapeutic opportunities [14]. Here, we applied a multiomics framework to longitudinal cerebrospinal fluid (CSF) samples from individuals who were cognitively unimpaired at baseline and subsequently developed cognitive impairment. By examining paired cognitively unimpaired (CU) or cognitively impaired (CI) states within the same participants, we identified dynamic changes in electrolytes, metabolites, lipids, and proteins that accompany cognitive decline. Importantly, these findings reveal molecular pathways beyond amyloid and tau that are altered during the earliest stages of cognitive impairment, highlighting new opportunities for biomarker discovery and the development of targeted interventions. Because amyloid and tau biomarkers were not used to define cognitive impairment in this cohort, the present study does not aim to identify Alzheimer's disease-specific molecular signatures. Rather, it seeks to generate hypotheses regarding molecular changes associated with the transition from cognitively unimpaired to cognitively impaired states.

METHODS

Ethics statement

Study protocols and consent forms were reviewed and approved by the Huntington Medical Research Institutes (HMRI) clinical review committee and the Institutional Review Board (HMRI# 33797). Written informed consent was obtained from each older adult recruited from the Pasadena area. We recruited older adults (>60 years) as part of an ongoing longitudinal brain-aging study in the Department of Neurosciences, Huntington Medical Research Institutes (HMRI), California. An overall clinical, neurological, and comprehensive neuropsychological assessment was performed to determine their cognitive status at baseline and was subsequently repeated for 2-3 years via a neuropsychological battery.

Diagnosis of cognitive performance

Participants were older adults over 60 years of age who were cognitively unimpaired (CU) at enrollment, not taking anticoagulant medications, and able to undergo magnetic resonance imaging (MRI). At the initial clinic visit, participants received a study briefing, provided a detailed medical history, and underwent a neurological examination. Cognitive function was assessed via the Mini-Mental State Examination (MMSE), Montreal Cognitive Assessment (MoCA), Clinical Dementia Rating (CDR), and Geriatric Depression Scale (GDS), followed by a comprehensive neuropsychological test

battery. The participants were monitored longitudinally, and those exhibiting cognitive decline were included in the study. The present analysis compares paired baseline and follow-up measurements within individuals and was not designed to model individual longitudinal trajectories or variable rates of cognitive decline. CU status was defined on the basis of neuropsychological performance within the expected range for age-matched peers. Conversion to CI was determined by performance at least 1.5 standard deviation below age norms on two or more non-memory tests within a specific cognitive domain, including memory, psychomotor speed, language, visuospatial skills, or executive function.

Inclusion and exclusion criteria

We included eight participants from our longitudinal cohort who transitioned from cognitively unimpaired (CU) status to cognitive impairment (CI) during follow-up. Inclusion required documented conversion based on longitudinal clinical assessments and neuropsychological testing. One participant met the criteria for Alzheimer's disease dementia,defined by a decline in Mini-Mental State Examination (MMSE) score, impairments ≥2.0 standard deviations below age-adjusted norms in multiple cognitive domains, and a clinically significant functional decline in activities of daily living. The remaining seven participants exhibited cognitive impairment without meeting dementia-level diagnostic thresholds but demonstrated an objective decline consistent with CI. The exclusion criteria included a history of major psychiatric illness, significant neurological conditions, or medical comorbidities that could confound the cognitive assessment.

Sample collection

Cerebrospinal fluid (CSF) was collected from all the participants after overnight fasting,centrifuged (3000 RPM, 20°C, 10 min) to remove cell debris, fractionated into 1 mL aliquots, and stored at -80°C until it was used for multiomics analysis.

Sample preparation

The samples were prepared via an automated liquid handling system. Recovery standards were added before the first quality control (QC) preparation step. The samples were first denatured with ethanol and EDTA and subsequently digested with trypsin to generate LC-MS amenable peptides. To remove the undigested matrix, dissociate metabolites bound to the matrix, and recover chemically diverse metabolites, the digest was extracted with a polar organic solvent mixture followed by centrifugation and supernatant transfer. The resulting extract was stored at 4°C until LC-MS analysis.

Quality Control and Data Assessment

Quality control (QC) samples, including pooled matrix samples, QC pooled plasma or HeLa cell extracts, and QC water blanks, were incorporated into each analytical batch to monitor and correct for technical variation. Hydrophilic and lipophilic internal standards were added to all samples to support data normalization and ensure measurement accuracy. Experimental samples were randomized across the platform, with pooled QC samples interspersed throughout the runs to evaluate analytical consistency. QC assessments demonstrated robust relative quantification and high reproducibility across samples and pooled controls. Hierarchical clustering on the basis of correlation distances (0.01-0.06) revealed strong sample relatedness. The distribution of coefficients of variation (CVs) for molecular intensities, displayed as a histogram, revealed that most peak areas presented CVs<0.2, indicating good precision in analyte detection. Principal component analysis (PCA) illustrated sample relationships in reduced-dimensional space, revealing biological heterogeneity,partial overlap between groups 1 and 2, and distinct multiomics profiles (**Supplementary Fig. 1**), providing additional validation of sample quality and analytical consistency.

Liquid Chromatography-Mass Spectrometry (LC-MS)

After trypsin digestion, the extracted samples were analyzed via ultrahigh-performance liquid chromatography (UHPLC)-tandem mass spectrometry (MS). The samples were analyzed via an electrospray ionization (ESI) source via a Thermo Vanquish UHPLC and a Thermo Scientific Q Exactive Plus mass spectrometer. The sample extract was separated via 2-dimensional UHPLC (RP-HILIC) via mobile phase gradients composed of water, acetonitrile, and isopropanol, with formic acid and ammonium acetate mobile phase additives. The data were acquired via segmented MS1 scans with fast polarity switching for quantification. The data were identified via data-dependent MS2 scans with retention-time-segmented precursor scans and dynamic exclusion. The mass analyzer was operated between 17,500 and 70,000 mass resolutions, covering a scan range of 80 to 1650 m/z.

LC-MS peak identification

The analyte data were collected via MS1-based relative quantification and MS^2-based identification. Ions were identified by matching data-dependent MS2 fragmentation spectra against theoretical and experimental species-specific proteomic, lipidomic, and metabolomic mass spectral libraries, respectively. After mass and retention time alignment and calibration,relative peak areas were extracted for identified ions based on matching MS1 mass-to-charge, retention time, and polarity. Peaks from the data-dependent MS2 fragmentation data were identified by matching to analyte libraries of experimental or theoretical spectra. Protein identification was performed via MSFragger software [15] with an appropriate species-specific protein sequence

database and a target-decoy false discovery rate (FDR) < 1%. Metabolite identification was performed via Thermo Compound Discoverer mzCloud Best Match Score > 80%, internal Dalton software with a dot product > 80% and more than 3 matching fragmentationions. Lipid identification was performed via Lipidex software [16-19] with a forward dot product >50%, a reverse dot product > 70%, and 2 or more matching fragment ions.

LC-MS relative quantification

The raw MS1 data were aligned using persistent background ions as lock masses. The MS^1 data retention time was aligned with a template run based on MS1 spectral correlations across run times. MS1 data were then calibrated for mass-to-charge ratio (m/z) based on all identified ions. Ion intensities are extracted by summing ion signals based on 5-ppm m/z and 1-minute tolerance around identified ions, followed by log10 transformation. Background ions were filtered based on their presence in the QC water samples. Ions were aggregated into molecule-level analytes by averaging (e.g., peptides into proteins). The outliers were omitted based on the correlation distance between each sample profile ($r < 0.8$). Intensity normalization was used to correct variable sample preparation and injection volumes. The run order and batch effects were corrected via statistical linear modeling. Relative intensities were statistically corrected for technical run order and batch effects, followed by mode-centering intensity normalization separately per biochemical class (electrolytes, metabolites, lipids, peptides). Multiple ion signals are averaged to form molecular-level relative quantifications. Molecular relative quantification data were analyzed via global data structure, differential analyte expression, and pathway enrichment.

Statistical and differential analyses and pathway enrichment

Differences in metabolites, lipids, and proteins between CUs and CIs were determined via paired nonparametric analysis (Wilcoxon signed-rank test) via GraphPad Prism. Because of the small sample size and the exploratory nature of this untargeted multiomics study, statistical significance was assessed using paired Wilcoxon signed-rank tests ($p < 0.05$, uncorrected). We recognize that the absence of multiple-testing correction increases the risk of false-positive findings; therefore, the results should be considered hypothesis-generating and interpreted with caution pending validation in independent cohorts. Differential associations were visualized via volcano plots, and global data trends were visualized via dimensionality reduction (PCA) and clustering plots. Multiomics pathway enrichment was statistically assessed via the Reactome pathway browser and ShinyGO 0.82. Correlation and network analyses of proteins were performed via MetaboAnalyst 6.0.

RESULTS

Clinical and demographic characteristics of the study participants

All eight participants included in this study were cognitively unimpaired (CU) at baseline and subsequently exhibited cognitive impairment (CI) at follow-up. The demographic data are summarized in **Table 1**, and Z scores from detailed neuropsychological (NP) examinations performed to determine the cognitive function of the study participants are listed in **Supplementary Table 1**.

Table 1. Demographic, and clinical data (p value -Wilcoxon signed rank test).

	Cognitively unimpaired (CU)	Cognitively Impaired (CI)	Change from CU (Mean ± SD)	P value
Demographic data, Mean ± SD (95% Confidence Interval)				
Age (years)	78.6 ± 8.4 (71.6-85.7)	83.3 ± 7.0 (77.4-89.1)	4.6 ± 3.5	
Female (%)	7/8 (87.5%)	7/8 (87.5%)	N/A	
Family history of dementia (%)	6/8 (75%)	6/8 (75%)	N/A	
ApoE4 status, CSF Biomarker, Mean ± SD (95% Confidence Interval)				
APOE4 carriers	3/8 (37.50%)	3/8 (37.50%)	N/A	
Aβ42 (pg/mL)	117.10 ± 27.17 (94.41-139.80)	136.10 ± 100.20 (52.37-219.90)	19.0 ± 81.5	0.8438
Tau (pg/mL)	375.4 ± 222.10 (189.70-561.10)	561.7 ± 432.00 (162.20-961.30)	116.1 ± 321.9	0.2188
Aβ42/Tau	0.41 ± 0.23 (0.22-0.60)	0.48 ± 0.55 (-0.3-0.99)	0.01 ± 0.53	0.9375

At the baseline visit, the participants had a mean age of 78.6 ± 8.4 years (range: 71.6–85.6; 95% CI), which increased to 83.2 ± 7.0 years (range: 77.4–89.1; 95% CI) at follow-up, corresponding to an average interval of 4.6 ± 3.5 years. The cohort included a greater proportion of women and participants with a family history of dementia. ApoE4 carriers represented 37.5% of the group. Although not statistically significant, follow-up assessments revealed trends toward higher total CSF tau, and a decreased Aβ42/tau ratio. Body mass index (BMI), fasting glucose, and lipid profiles remained largely unchanged between the baseline visit and the follow-up visit (**Table 2**).

Table 2. BMI, fasting blood glucose, and lipids.

	Cognitively unimpaired (CU)	Cognitively Impaired (CI)	Change from CU (%)
BMI	26.01 ± 6.3 (19.22-38.59)	24.69 ± 9.2 (18.32-46.29)	-5.3
Glucose (mg/dL)	83.14 ± 7.9 (71.0-92.0)	78.75 ± 9.3 (67.0-95.0)	-5.6
TG (mg/dL)	64.0 ± 14.9 (51.0-88.0)	63.38 ±15.6 (47.0-100.0)	-1.0
Cholesterol (mg/dL)	192.1 ± 27.5 (147.0-219.0)	192.8 ± 39.5 (148.0-256.0)	0.4
HDL (mg/dL)	79.29 ± 19.3 (58.0-105.0)	78.88 ± 13.9 (60.0-98.0)	-0.5
LDL (mg/dL)	105.4 ± 16.8 (81.0-129.0)	107.9 ± 34.7 (77.0-175.0)	2.3
VLDL (mg/dL)	12.43 ± 2.9 (10.0-17.0)	12.63 ± 3.2 (9.0-20.0)	1.6

Differential Cerebrospinal Fluid Metabolites associated with Cognitive Impairment

Using LC-MS, we identified a total of 1,478 cerebrospinal fluid (CSF) analytes, comprising 4 electrolytes, 202 metabolites, 343 lipids, and 929 proteins. We compared analyte profiles in each molecular class between cognitively unimpaired (CU) and cognitively impaired (CI) states within the same participants (n = 8). Our exploratory analysis identified 109 molecular groups that differed between the cognitively unimpaired and cognitively impaired states, including 1 electrolyte, 5 metabolites, 33 lipids, and 70 proteins, associated with the transition to cognitive impairment (**Supplementary Table 2**).

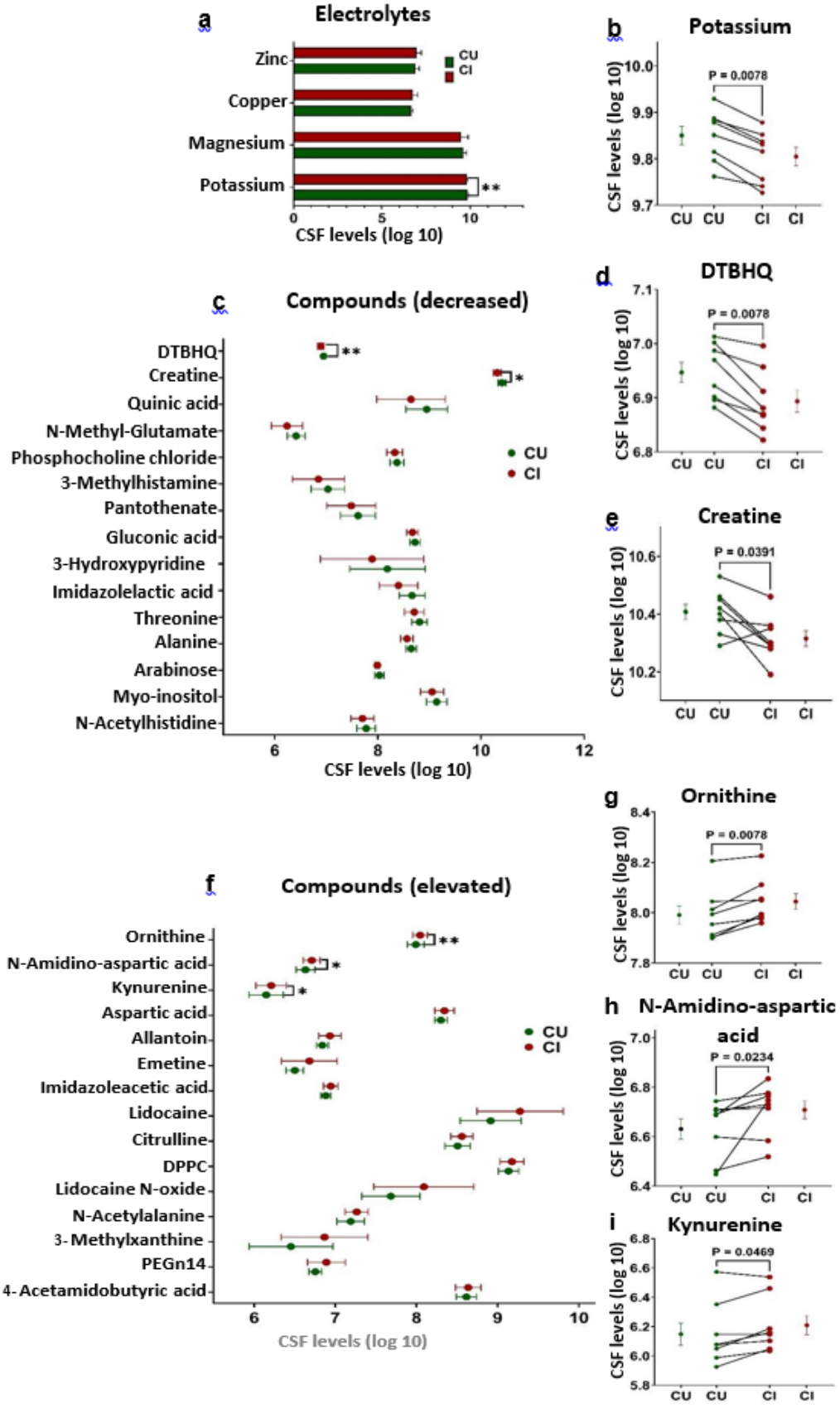
Electrolyte alterations in cognitive impairment

Among the four electrolytes detected in cerebrospinal fluid (CSF), potassium (K^+), magnesium (Mg^{2+}), copper (Cu^{2+}), and zinc (Zn^{2+}) (**Fig. 1a**), potassium levels significantly decreased ($p = 0.0078$) as participants progressed from the cognitively unimpaired (CU) state to the cognitively impaired (CI) state (**Fig. 1b**). No significant changes were observed for magnesium, copper, or zinc. The reduction in CSF potassium suggests potential disturbances in neuronal excitability and ion homeostasis that may accompany early cognitive decline.

CSF compounds associated with cognitive impairment

We analyzed 202 metabolites in cerebrospinal fluid (CSF) to identify metabolic changes accompanying the transition from cognitively unimpaired (CU) to cognitively impaired (CI) states. Of these, five compounds were significantly altered. The 15 compounds exhibiting the greatest decreases in CSF with cognitive impairment are shown in **Fig. 1c**, with 2,5-di-tert-butylhydroquinone (DTBHQ) and creatine showing the most pronounced reductions, suggesting potential impairments in antioxidant defense and cellular energy metabolism (**Fig. 1d, e**). In contrast, the 15 compounds displaying the greatest increases are presented in **Fig. 1f,** including ornithine, N-amidino-aspartic acid, and kynurenine, whose elevated levels reflect perturbations in amino acid metabolism, the urea cycle, and the kynurenine pathway, respectively (**Fig. 1g-i**). These results reveal selective metabolic alterations associated with early cognitive decline and indicate that disruptions in energy homeostasis, oxidative stress, and neuroactive amino acid-derived metabolites may contribute to the molecular mechanisms underlying cognitive impairment.

Figure 1. Cerebrospinal fluid (CSF) levels of electrolytes and compounds in cognitively unimpaired (CU) and cognitively impaired (CI) participants. (a) The levels of four electrolytes detected in the CSF of CU and CI participants. (b) Potassium levels in individual participants at the CU and CI stages. The data represent the means ± SDs. (c) CSF levels of the top 15 compounds decreased with cognitive impairment. (d-e) CSF levels of 2,5-di-tert-butylhydroquinone (d) and creatine (e) in individual participants at the CU and CI stages. The data represent the means ± SDs. (f) CSF levels of the top 15 compounds that increased with cognitive impairment. (g) CSF levels of ornithine, (h) N-amidino-aspartic acid, and (i) kynurenine in individual participants at the CU and CI stages. The data represent the means ± SDs.



Lipid classes and species in CSF and their associations with cognitive impairment

To explore lipid alterations accompanying cognitive decline, we first assessed the enrichment of lipid classes via WikiPathways. Phosphatidylcholines (76 species) and sphingomyelins (44 species) emerged as the most abundant lipid classes in the CSF of the study participants, followed by lysophosphatidylcholines, phosphatidylethanolamines, acylcarnitines, lysophosphatidylethanolamines,and plasmenyl phosphatidylethanolamines (**Fig. 2a**).

Overall lipid alterations with cognitive impairment

Among the 343 lipid species detected, 33 were significantly associated with cognitive impairment. These categories spanned five major lipid categories, namely, fatty acyls, glycerolipids, glycerophospholipids, sterol lipids, and sphingolipids, each revealing distinct patterns of dysregulation in the transition from CU to CI.

Fatty acyls

Among the 54 fatty acyl species identified in CSF, the top 15 fatty acyls showing decreases are presented in **Fig. 2b**. Four fatty acyl species were significantly reduced in association with cognitive impairment: myristic acid, docosanamide, oleamide, and erucamide (**Fig. 2c-f**). Notably, oleamide and erucamide are sleep-regulating molecules, and their decreases may reflect impaired sleep-wake regulation, a process strongly linked to memory consolidation and Alzheimer's disease pathology. In contrast, most fatty acyls exhibiting increasing trends were acylcarnitines (**Fig. 2g**), which is consistent with altered mitochondrial fatty acid transport and disrupted β-oxidation in individuals with cognitive impairment. Lauroylcarnitine was the only fatty acyl that significantly increased (**Fig. 2h**), whereas acylcarnitine 12:0, linoleic acid, and palmitoylcarnitine also tended to increase (**Fig. 2g**). Elevated acylcarnitines have been associated with mitochondrial dysfunction, energy deficits, and neuroinflammation, suggesting that shifts in CSF fatty acyl profiles may contribute to the metabolic stress underlying cognitive decline.

Glycerophospholipids

A total of 179 glycerophospholipid species were identified in CSF, of which 11 were significantly elevated and 7 were significantly reduced in association with cognitive impairment. The most prominent decreases were observed in phosphatidylethanolamines (PEs) and their deacylated derivatives, lysophosphatidylethanolamines (LysoPEs), suggesting perturbations in membrane integrity and remodeling. The top 15 glycerophospholipids whose levels decreased with cognitive impairment are shown in **Fig. 3a**. Specific reductions were detected in PC 38:7, PE40:7, LysoPE 18:2, PI 36:4, PC 39:7, oxidized PC (OH) OH 43:6, and LysoPE 22:6 (**Fig. 3b-e**), several of which are enriched in neuronal membranes and involved in synaptic function. Conversely, several glycerophospholipids are elevated in cognitively impaired individuals.These included phosphatidylcholines(PCs),
lysophosphatidylcholines (LysoPCs), and plasmalogen species, such as plasmenyl-PCs and plasmenyl-PEs (**Fig. 3f**). Notably, plasmalogens are ether-linked phospholipids that are abundant in myelin and synaptic vesicles, and their increase may represent either a compensatory mechanism to preserve membrane stability or a consequence of altered lipid remodeling in the diseased state. The significantly increased lipids included Plasmenyl-PC P-36:4, LysoPC (0:0/18:0), PC44:5,1-Stearoyl-sn-Glycero-3-Phosphocholine, Plasmenyl-PC O-36:4, PC 46:9, PC 34:0,

Glycerolipids

Four glycerolipids were detected, including three diacylglycerols (DGs 34:1, 34:2, 36:2), which increased in CI, and one triacylglycerol (TG 54:4), which decreased (**Fig. 3k**). Diacylglycerols are important membrane-derived signaling lipids implicated in synaptic plasticity and neuroinflammatory cascades, suggesting that their dysregulation may contribute to impaired neuronal communication in CI.

Sterol lipids

Sterol metabolism was also perturbed, with 12 sterol lipids fluctuating between the CU and CI states. Notably, the levels of sex steroids (testosterone), glucocorticoids (cortisol,cortisone), and bile acids (cholic and taurocholic acids) decreased, whereas cholesterol, corticosterone, glycochenodeoxycholic acid, and other secondary bile acids increased (**Fig. 3l, 3m**). The significant reduction in testosterone is consistent with prior studies linking androgen decline to cognitive deterioration, whereas elevated bile acids suggest a potential gut-brain metabolic axis contributing to neurodegeneration [20,21].

Figure 2. Lipid class enrichment and cerebrospinal fluid (CSF) fatty acyl profiles in cognitively unimpaired (CU) and cognitively impaired (CI) participants. (a) Distribution of lipid classes in CSF associated with cognitive status. (b) CSF levels of the top 15 fatty acyl compounds decreased with cognitive impairment. (c) CSF levels of myristic acid, (d) docosanamide, (e) oleamide, and (f) erucamide in individual participants at the CU and CI stages. The data represent the means ± SDs. (g) CSF levels of the top 15 fatty acyl compounds increased with cognitive impairment. (h) CSF levels of lauroylcarnitine in individual participants at the CU and CI stages. The data represent the means ± SDs.

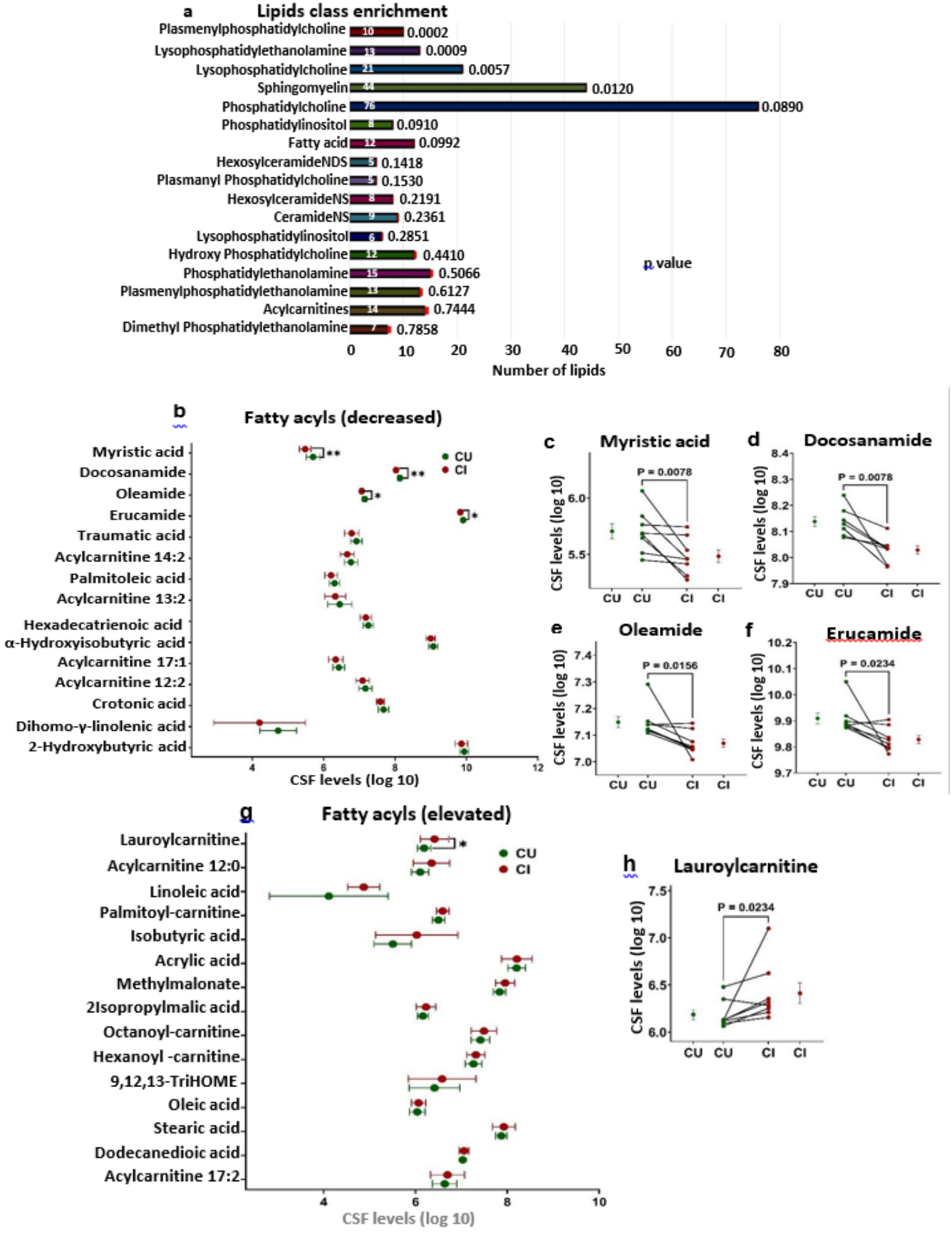
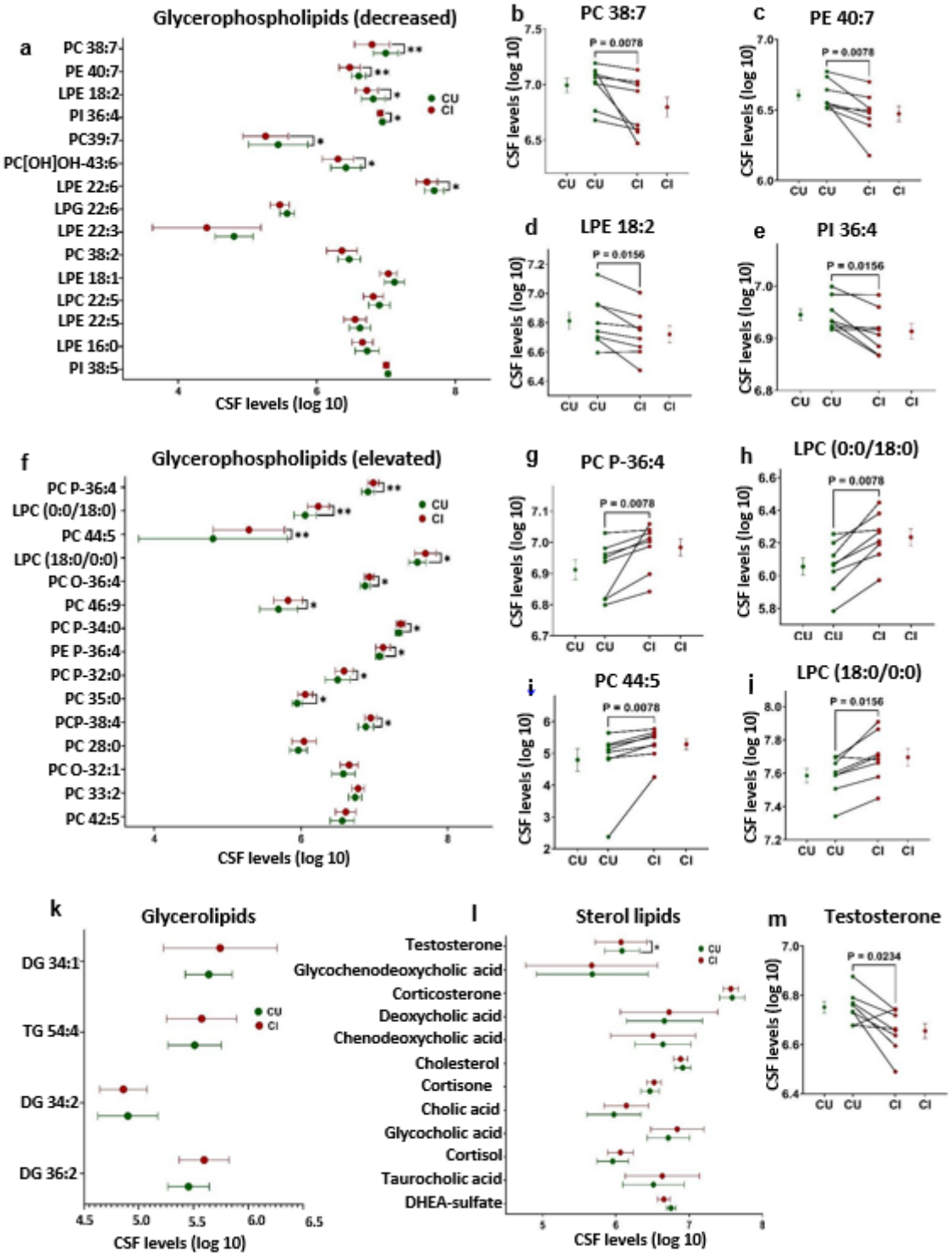


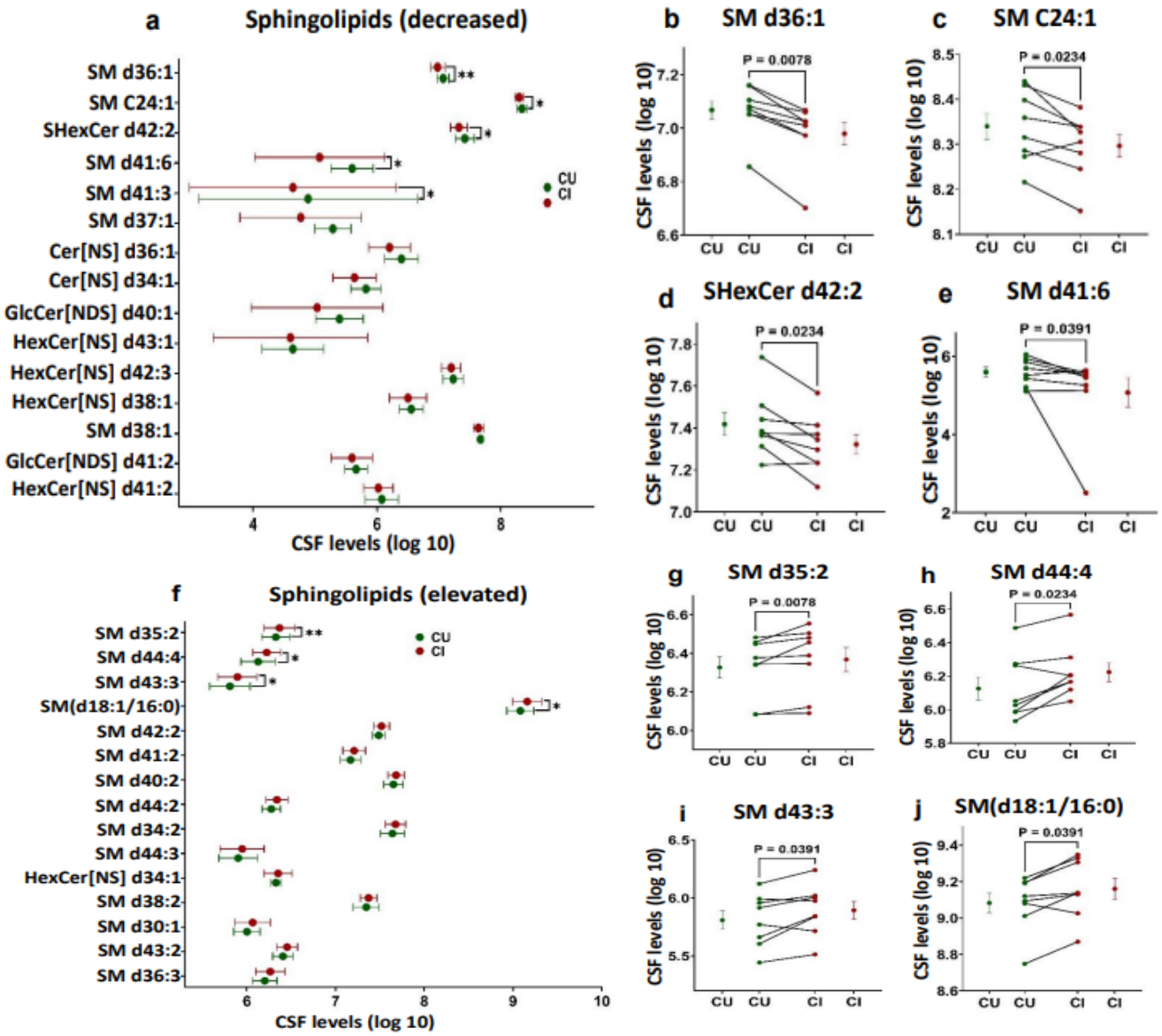
Figure 3. Cerebrospinal fluid (CSF) levels of glycerophospholipids, glycerolipids, and sterol lipids in cognitively unimpaired (CU) and cognitively impaired (CI) participants. (a) Comparison of CSF levels of the top 15 glycerophospholipids whose levels decreased with cognitive impairment. (b-e) CSF levels of (b) PC 38:7, (c) PE 40:7, (d) LPE 18:2, and (e) PI 36:4 in the individual participants at the CU and CI stages. The data represent the means ± SDs. (f) CSF levels of the top 15 glycerophospholipids increased with cognitive impairment. (g-j) CSF levels of PC P-36:4 (g), LPC (0:0/18:0) (h), PC 44:5 (i), and LPC (18:0/0:0) (j) in individual participants at the CU and CI stages. The data represent the means ± SDs. (k) CSF levels of four glycerolipids in the CSF of CU and CI participants. (l) CSF levels of sterol lipids in the CSF of CUs and CIs. (m) CSF testosterone levels in individual participants at the CU and CI stages. The data represent the means ± SDs.



Sphingolipids

Among the 71 sphingolipids identified, 38 decreased and 33 increased with cognitive impairment. The top 15 sphingolipids whose levels decreased or increased with cognitive impairment are shown in **Fig. 4a** and **4f**. Among the significantly reduced species were four sphingomyelins (SM d36:1, SM C24:1, SM d41:6, SM d41:3) and one hexosylceramide (SHexCerd42:2) (**Fig. 4b-e**). In contrast, several sphingomyelins (e.g., SM d35:2, SM d44:4, SM d43:3, and SM d18:1/16:0) were significantly elevated (**Fig. 4g-j**). Given the vital role of sphingolipids in membrane microdomain organization, myelination, and cell signaling, these bidirectional shifts may reflect complex remodeling of lipid rafts and synaptic vesicle dynamics during cognitive decline.

Figure 4. Cerebrospinal fluid (CSF) sphingolipid alterations in cognitively unimpaired (CU) and cognitively impaired (CI) participants. (a) CSF levels of the top 15 sphingolipids decreased with cognitive impairment. (b-e) CSF levels of SM d36:1 (b), SM C24:1 (c), SHexCer d42:2 (d), and SM d41:6 (e) in individual participants at the CU and CI stages. The data represent the means ± SDs. (f) CSF levels of the top 15 sphingolipids whose levels increased with cognitive impairment. (g-j) CSF levels of SM d35:2 (g), SM d44:4 (h), SM d43:3 (i), and SM (d18:1/16:0) (j) in individual participants at the CU and CI stages. The data represent the means ± SDs.



Summary of lipid alterations

Together, these findings highlight widespread dysregulation of lipid metabolism in CSF during the transition from CU to CI. Alterations involved pathways linked to sleep regulation (oleamide), mitochondrial function, and energy homeostasis (acylcarnitines, PEs), synaptic signaling (diacylglycerols, PCs), neurosteroid balance (testosterone, cortisol), bile acid metabolism, and membrane microdomain integrity (sphingolipids). These lipidomic shifts point to diverse metabolic and signaling disturbances that may contribute to impaired neuronal function and synaptic vulnerability in Alzheimer's disease and related dementias.

Evaluation of CSF proteins associated with cognitive impairment

Among the 929 proteins detected in CSF, 70 were significantly altered between the CU and CI states (**Supplementary Table 3**). Cognitive impairment was associated with reduced CSF levels of 23 proteins (top 15 shown in **Fig. 5a**), of which the most prominent reduction was observed in ephrin-A1 (P20827), reticulocalbin-2 (Q14257), chondroadherin (O15335), chymotrypsinogen A (P00766), polypeptide N-acetylgalactosaminyltransferase 16 (Q8N428), and amyloid-β precursor protein (P05067) (**Fig. 5b-g**). Conversely, 31 additional proteins were significantly elevated in CI (top 15 shown in **Fig. 5h**), of which prominent increases were observed in the levels of matrilin-2 (O00339), lumican (P51884), gelsolin (P06396), desmoglein-2 (Q14126), protocadherin-17 (O14917), coagulation factor XIII B chain (P05160), TGF-β receptor type 3 (Q03167), non-secretory ribonuclease (P10153), ribonuclease inhibitor (P13489), and VPS10 domain-containing receptor SorCS3 (Q9UPU3) (**Fig. 5i-r**).

Pathway enrichment analysis revealed that extracellular matrix (ECM) proteins, cell-surface molecules, and transmembrane proteins, which are collectively categorized as cell-matrix adhesion proteins, were the most prominent groups associated with CI (**Table 3**). Specifically, 18 proteins within this category exhibited cognitive state-dependent changes. In the CI state, the CSF levels of lumican, matrilin-2, desmoglein-2, protocadherin-17, glycoprotein NMB, vasorin, SorCS3, thrombospondin-4, neuroligin-1, and noelin were significantly elevated. In contrast, ephrin-A1, chondroadherin, amyloid-β precursor protein, cell adhesion molecule 3, neural cell adhesion molecule 1, LINGO3, and sodium channel subunit β-2 were decreased.

Together, these findings suggest that cognitive decline is accompanied by pronounced remodeling of the extracellular matrix and alterations in cell-cell and cell-matrix adhesion signaling pathways, processes that may influence synaptic stability, neuroplasticity, and neuronal survival.

Biological pathway enrichment analyses

To gain deeper insight into the molecular processes associated with cognitive impairment, we performed pathway enrichment analysis via ShinyGO with STRING database integration. Amyloid fibril formation, regulation of the response to stimuli, signaling, cell communication,localization, multicellular organismal processes, intracellular signal transduction, and cell death were found to be the major significant pathways altered in the CSF of CI participants (**Fig. 6a**).These findings underscore the diverse molecular disturbances accompanying the transition from CU to CI.

The enrichment of cellular compartments revealed strong representation of proteins localized to the extracellular space, extracellular vesicles (including exosomes), and plasma membrane, with additional enrichment in the endomembrane system, cytoplasmic vesicles,extracellular matrix (ECM), and intrinsic membrane proteins (**Fig. 6b**). Stratified analysis revealed that proteins decreased in CI participants were enriched in the endoplasmic reticulum (ER) lumen and ECM, suggesting compromised protein folding and matrix integrity. In contrast, proteins enriched in CI were preferentially enriched in sarcomeres, receptor complexes, plasma membrane protein complexes, the cell surface, and the early endosome membrane (**Supplementary Table 4**), indicating the dynamic remodeling of vesicle trafficking and signaling interfaces.

Chromosomal enrichment analysis revealed the greatest number of genes encoding differentially expressed proteins on chromosome 1 (n = 7). Individual genes were mapped to chromosomes8(matrilin-2),10(SorCS3),13(protocadherin-17), and X (SH3 domain-binding glutamic acid-rich-like protein), whereas genes associated with neurodegenerative processes included MAPT on chromosome 17 and APP on chromosome 21 (**Fig. 6c**).

Finally, molecular function analysis revealed significant enrichment for cell adhesion molecule (CAM) binding, involving proteins encoded by 11 genes. These findings suggest that alterations in protein–protein interactions at synaptic and extracellular interfaces may contribute to molecular pathways associated with cognitive impairment.

Figure 5. Cerebrospinal fluid (CSF) protein alterations associated with cognitive impairment. (a) The top 15 proteins whose expression decreased with cognitive impairment. (b-g) CSF levels of ephrin-A1 (P20827) (a), reticulocalbin 2 (Q14257) (c), chondroadherin (O15335) (d), chymotrypsinogen A (P00766) (e), polypeptide N-acetylgalactosaminyltransferase 16 (Q8N428), (f) and amyloid beta precursor protein (P05067) (g) in individual participants at the CU and CI stages. The data represent the means ± SDs. (h) The expression of the top 15 proteins significantly increased with cognitive impairment. (i-r) CSF levels of matrilin-2 (O00339) (i),lumican (P51884) (j), gelsolin (P06396) (k), desmoglein 2 (Q14126) (l), protocadherin 17 (O14917) (m), coagulation factor XIII B chain (P05160) (n), transforming growth factor beta receptor 3 (Q03167) (o), non-secretory ribonuclease (P10153) (p), ribonuclease inhibitor (P13489) (q) and VSP10 domain-containing receptor SorCS3 (Q9UPU3) (r) in individual participants at the CU and CI stages. The data represent the means ± SDs.

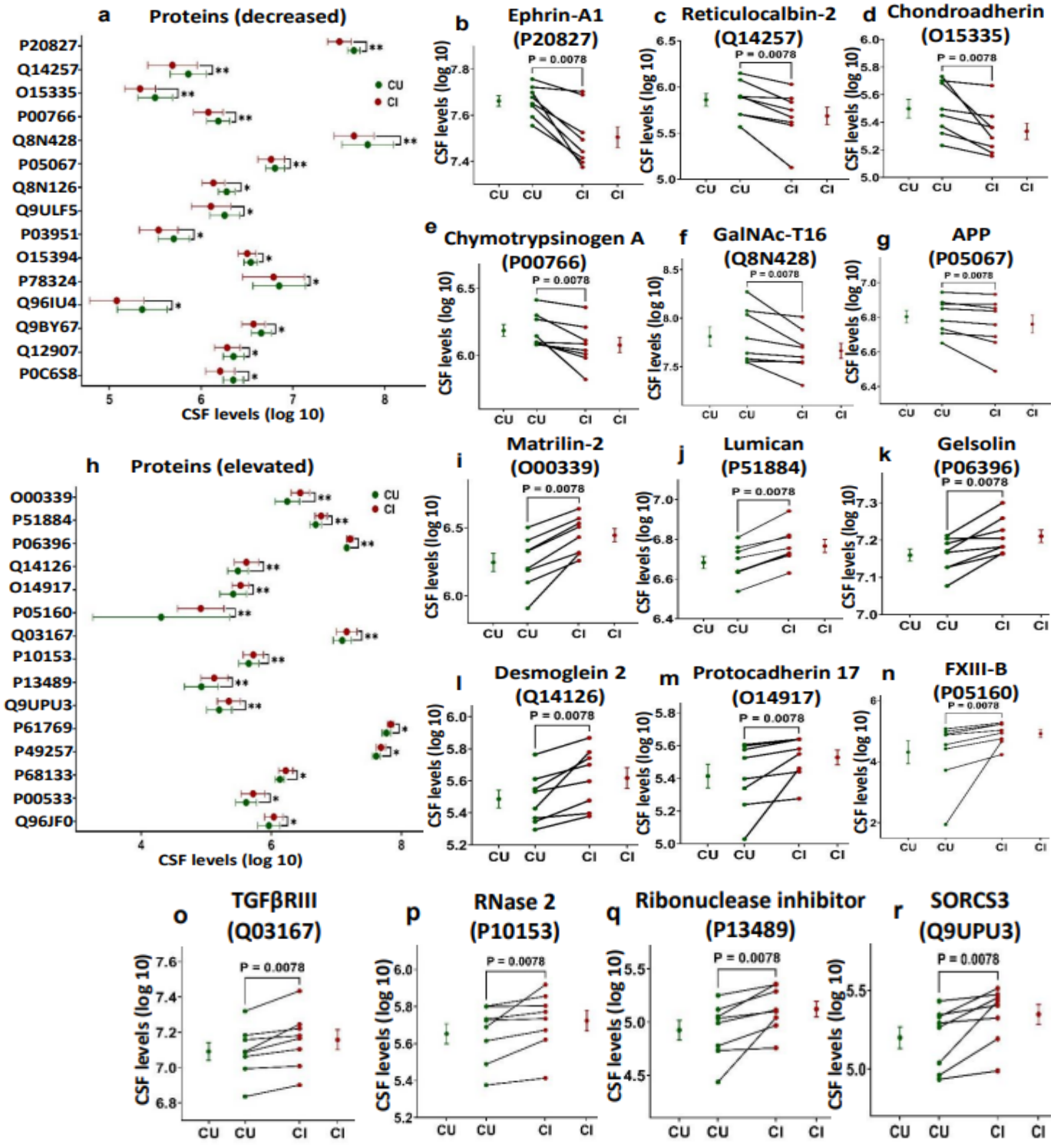
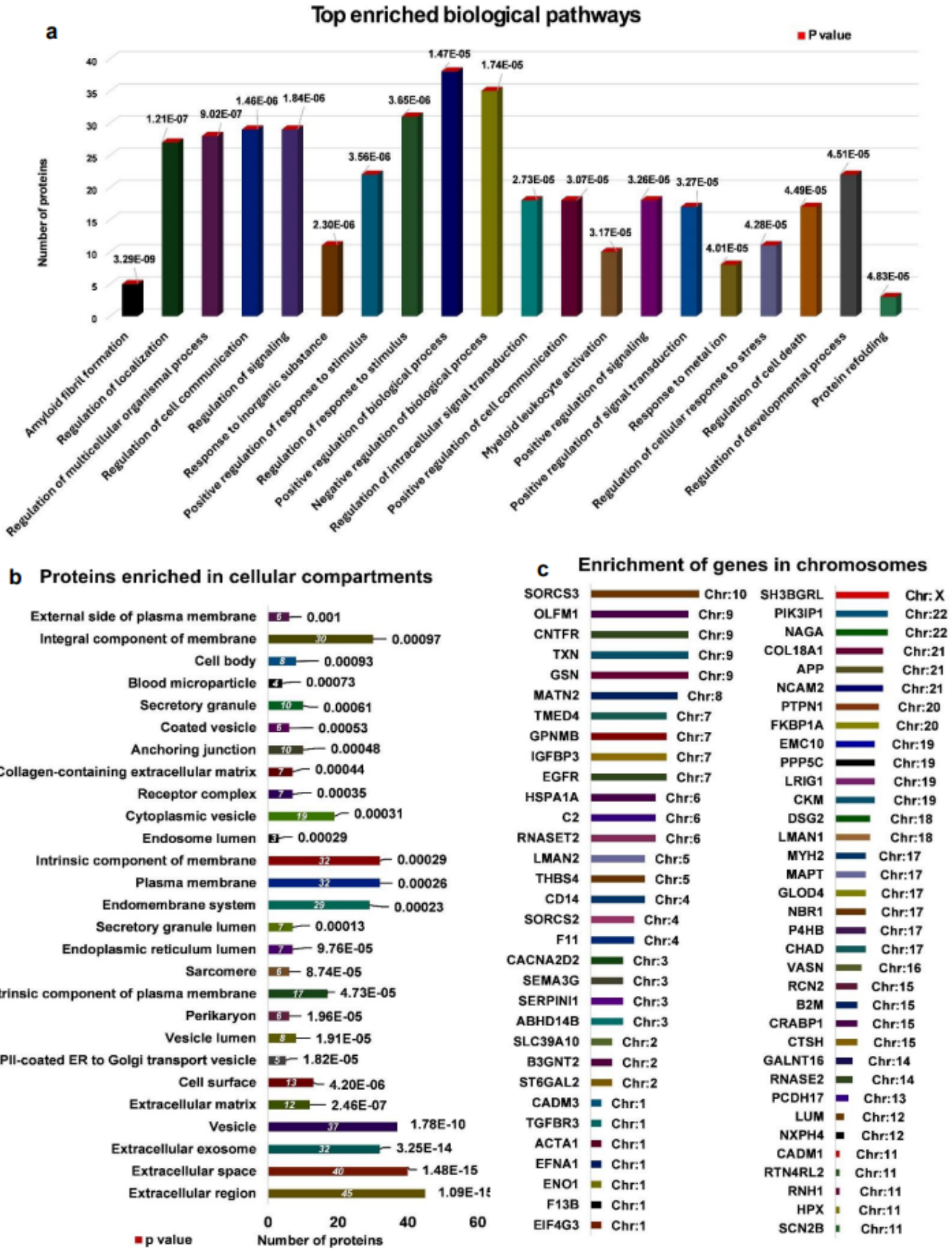


Figure 6. Enrichment analysis of biological pathways, cellular compartments, and chromosomal localization of proteins. (a) Top biological pathways associated with cognitive status, ranked by statistical significance (p values). (b) Enrichment of proteins in distinct cellular compartments, showing both significance (p values) and the number of proteins enriched in each compartment. (c) Chromosomal localization of genes corresponding to proteins detected in study participants.



Correlation and network analysis

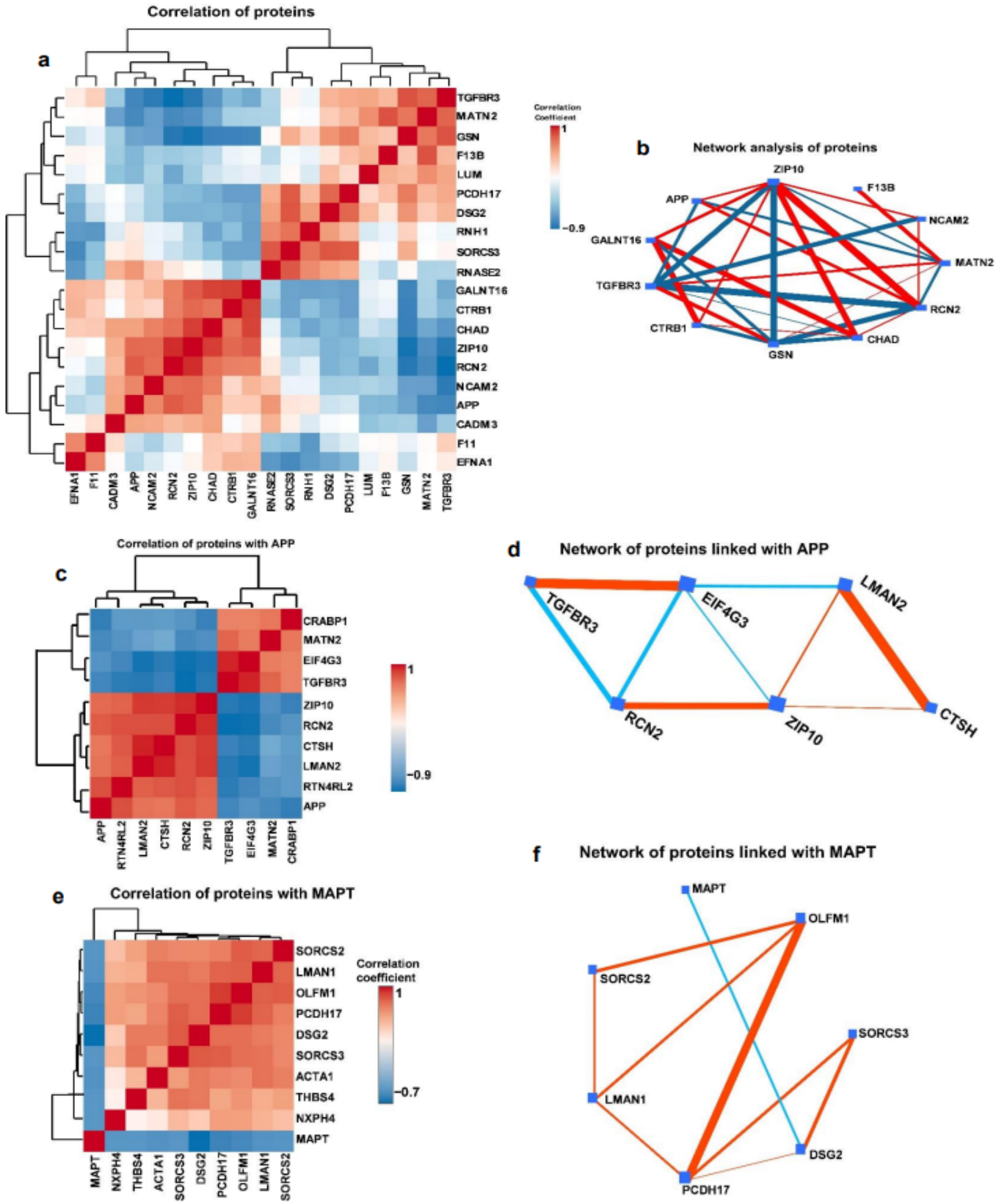
To investigate the interrelationships among CSF proteins altered with cognitive impairment, we performed Spearman correlation analyses separately for proteins that decreased or increased in the CI state (**Supplementary Figs. 2-3**). Among the top 20 proteins, lumican (P51884), matrilin-2 (O00339), gelsolin (P06396), protocadherin-17 (O14917), and desmoglein-2 (Q14126) were strongly positively correlated with each other and negatively correlated with amyloid-β precursor protein (APP, P05067), ephrin-A1 (P20827), chymotrypsinogen A (P00766), reticulocalbin-2 (Q14257), zinc transporter ZIP10 (Q9ULF5), and chondroadherin (O15335) (**Fig. 7a**). Network analysis highlighted additional relationships, including a strong positive correlation of ZIP10 with reticulocalbin-2 and chondroadherin and a negative correlation with gelsolin and transforming growth factor beta receptor type 3 (TGFBR3, Q03167). Reticulocalbin-2 was negatively associated with TGFBR3, emphasizing potential regulatory interactions among these proteins (**Fig. 7b**).

Focusing on APP, correlation analysis revealed positive associations with reticulon-4 receptor-like 2 (Q86UN3), VIP36 (Q12907), pro-cathepsin H (P09668), reticulocalbin-2 (Q14257),and ZIP10 (Q9ULF5) and negative correlations with cellular retinoic acid-binding protein 1 (P29762), matrilin-2 (O00339), eukaryotic translation initiation factor 4 gamma 3 (O43432), and TGFBR3 (Q03167) (**Fig. 7c**). Interestingly, network analysis indicated that APP did not display significant correlations with several other top proteins (**Fig. 7d**), suggesting selective connectivity within the CI-associated protein network.

For the microtubule-associated protein A0A7P0T936, negative correlations were observed with multiple cell adhesion and extracellular matrix proteins, including desmoglein-2,protocadherin-17, noelin (Q99784), ERGIC-53 (P49257), SorCS2 (Q96PQ0), SorCS3 (Q9UPU3),alpha-actin (P68133), thrombospondin-4 (P35443), and neurexophilin-4 (O95158) (**Fig. 7e**).Notably, microtubule-associated proteins also exhibited a direct negative correlation with desmoglein-2 (**Fig. 7f**), highlighting a potential link between cytoskeletal regulation and cell adhesion processes during cognitive decline.

Overall, these correlation and network analyses revealed tightly coordinated modules of proteins whose abundance changes were interrelated during cognitive impairment, suggesting mechanistic links between extracellular matrix remodeling, synaptic adhesion, and cytoskeletal integrity.

Figure 7. Correlation and network analyses of cerebrospinal fluid (CSF) proteins associated with cognitive status. (a) Correlation matrix of the top 20 proteins significantly associated with cognition (ranked by p value). (b) Network analysis of the top proteins, where red and blue lines indicate positive and negative correlations, respectively; line intensity reflects correlation strength. (c) Correlations of amyloid-beta precursor protein (P05067) with other proteins. (d) Network analysis highlighting proteins most strongly connected to amyloid-beta precursor protein. (e) Correlations of microtubule-associated protein tau (A0A7P0T936) with the top nine significant proteins. (f) Network analysis showing proteins most strongly linked to the microtubule-associated protein tau.



DISCUSSION

In this study, we applied an integrative multiomics approach to cerebrospinal fluid (CSF) from cognitively unimpaired (CU) older adults who subsequently transitioned to a cognitively impaired (CI) state. By simultaneously profiling electrolytes, metabolites, lipids, and proteins, we captured a comprehensive molecular landscape associated with early cognitive decline, many of which have not been previously reported in Alzheimer's disease (AD) research (**Table 5**). Our findings reveal previously unrecognized alterations in CSF composition that may provide novel mechanistic insights into the earliest stages of neurodegenerative disease, particularly Alzheimer's disease (AD).

Electrolytes and cognitive function

Among electrolytes, a notable decrease in CSF potassium (K^+) was observed in CI participants. Potassium is essential for maintaining neuronal membrane potential and regulating synaptic transmission, which are critical for memory, learning, and overall cognitive function [22,23]. Reduced CSF K^+ levels may reflect subtle impairments in neuronal excitability and network synchronization, highlighting a potential early contributor to the cognitive decline that has rarely been documented in human CSF studies.

Metabolites and metabolic dysregulation

Our metabolomic profiling of 202 compounds revealed significant alterations in five molecules: 2,5-di-tert-butylhydroquinone (DTBHQ), creatine, ornithine, N-amidino-aspartic acid, and kynurenine. Among these, DTBHQ and creatine were decreased in cognitively impaired (CI) participants, suggesting early disruption of antioxidant defenses and mitochondrial energy metabolism. Creatine, in particular, has been well studied in Alzheimer's disease (AD) models, where it supports ATP regeneration, protects against oxidative stress, and mitigates amyloid-β toxicity [24-26].

In contrast, increases in ornithine, N-amidino-aspartic acid, and kynurenine indicate less characterized pathways of metabolic dysregulation in CI. Ornithine, a key intermediate in the urea cycle, has not been widely linked to AD but may contribute to cognitive decline through hyperactivation of astrocytic ammonia clearance, leading to excess GABA, hydrogen peroxide, and neurotoxic byproducts [27-29]. N-Amidino-aspartic acid (a form of D-aspartic acid), which is critical for synaptic plasticity and neurodevelopment [30,31], modulates NMDA receptor signaling but has not previously been reported in CSF from AD or CI cohorts. Its elevation suggests a potential novel mechanism of NMDAR dysregulation in early disease. In contrast, kynurenine and the kynurenine pathway have been implicated in AD and neuroinflammation, with prior studies showing elevated CSF kynurenine specifically in AD participants [32,33].

Together, these findings distinguish between established metabolites such as creatine and kynurenine, which validate known pathways in AD, and emerging candidates such as ornithine and N-amidino-aspartic acid, which may represent novel molecular links between amino acid metabolism, excitatory neurotransmission, and early cognitive impairment.

Lipidomic shifts in individuals with cognitive impairment

Our lipidomic profiling revealed broad alterations across multiple lipid classes, including fatty acyls, glycerolipids, glycerophospholipids, sphingolipids, and sterols, underscoring lipid metabolism as a central axis of early cognitive decline. Several of these changes align with established mechanisms in Alzheimer's disease (AD), whereas others point to previously unrecognized lipid species that may represent candidate molecules associated with cognitive decline.

Among the established lipid alterations in AD, myristic acid has been linked to brain aging, systemic inflammation, and GABAergic dysfunction,processes that can accelerate neurodegeneration [34-36]. Similarly, disruptions in glycerolipids have been reported in both AD and mild cognitive impairment (MCI), with altered glycerolipid metabolism proposed as an early event in AD progression [37,38]. In our study, elevated diacylglycerols (DAGs) in cognitively impaired (CI) participants suggest perturbed second messenger signaling, which is consistent with prior evidence of protein kinase C dysregulation [39]. Reductions in the levels of phosphatidylcholines (PCs), phosphatidylethanolamines (PEs), plasmalogens,and phosphoinositides (PIs) further highlight impaired neurotransmission, membrane integrity, and amyloid processing [40,41]. Low PC levels, particularly those containing DHA, have been consistently associated with increased dementia risk, whereas plasmalogen deficiency is linked to Aβ accumulation and impaired synaptic function [42-44]. Likewise, altered cholesterol and sterol levels, including testosterone levels, as well as sphingolipid dysregulation, have been implicated in synaptic failure and neurodegeneration in AD.

In contrast, our data identify several novel lipid candidates not extensively reported in the context of AD or CI. Fatty acyl primary amides, including docosanamide, oleamide, and erucamide, exhibit neuroprotective, anti-inflammatory, and cholinergic-modulating properties [45-48], suggesting potential compensatory mechanisms that may counteract neurodegenerative stress. The fatty acid primary amide oleamide, first described in preclinical studies, has subsequently been shown to be a potent sleep-inducing molecule that regulates sleep via its effects on serotonin and GABA receptors, enhancing cannabinoid function and inactivating GAP junctions [49-52]. The decrease in oleamide and related compounds in the CSF of CI participants suggests

a significant role of sleep in cognitive function. Elevated levels of lauroylcarnitine, a mitochondrial metabolite that supports fatty acid transport and energy metabolism, may represent a novel neurotrophic factor in early cognitive decline [53-56]. These findings extend prior work by implicating lesser-studied lipid mediators in CSF as candidate biomarkers and molecular correlates of CI.

In summary, our study confirms known lipid derangements in AD, such as deficits in phosphatidylcholine, plasmalogens, and sphingolipids, while also revealing novel lipid species—oleamide, erucamide, docosanamide, and lauroylcarnitine—that have not been systematically investigated in AD. Together, these results position lipid metabolism at the crossroads of energy failure, membrane remodeling, and inflammatory signaling and highlight new molecular avenues for biomarker discovery and therapeutic intervention.

Protein alterations and extracellular matrix remodeling

Proteomic analysis revealed 70 proteins significantly altered in association with cognitive impairment, highlighting widespread remodeling of the extracellular matrix (ECM) and cell-cell communication pathways. Several of these proteins map onto established mechanisms in Alzheimer's disease (AD), whereas others represent novel candidates not previously reported in human CSF during early cognitive decline.

Among the established AD-related proteins, ephrin-A1 (EphA1) has been genetically and functionally linked to AD, with mutations influencing receptor signaling, neuroinflammation, and blood–brain barrier integrity [57]. Chondroadherin (CHAD), a structural ECM protein that contributes to the formation of perineuronal nets (PNNs), regulates synaptic plasticity and connectivity; its disruption has been associated with impaired neuronal resilience and AD progression [58,59]. The amyloid precursor protein (APP) remains central to AD pathology, as aberrant processing generates amyloid-β (Aβ) peptides that aggregate into plaques, driving synaptic dysfunction and neurodegeneration [60]. Reticulocalbin-2 (RCN2), a calcium-binding protein, contributes to calcium homeostasis and mitochondrial stability, and its dysregulation has been implicated in neuronal vulnerability through calcium overload and mitochondrial apoptosis [61]. Together, these changes reinforce known pathways involved in AD pathogenesis, including synaptic adhesion deficits, calcium dysregulation, and Aβ pathology.

In contrast, our data also highlights novel ECM and adhesion-related proteins not extensively studied in the context of AD. Elevated lumican, matrilin-2, desmoglein-2,protocadherin-17, and noelin levels suggest active remodeling of the ECM and altered synaptic adhesion in CI. These proteins are known regulators of structural plasticity and intercellular communication in other biological contexts, but their presence and dysregulation in CSF during early cognitive decline have not been reported. Their emergence in our dataset points to potential mechanisms that warrant further study of ECM remodeling that may shape neuronal connectivity and resilience in prodromal stages of disease.

In summary, our findings both validate established AD-related alterations, including EphA1, CHAD, APP, and RCN2, and reveal novel ECM components and adhesion proteins that may represent early molecular signatures of CI. This duality underscores the ECM as a dynamic and underappreciated regulator of synaptic plasticity, amyloid deposition, and neuronal health while also expanding the landscape of candidate biomarkers and therapeutic targets for early intervention.

Integrated pathways and mechanistic insights

Enrichment analyses revealed that altered proteins are predominantly associated with extracellular vesicles, exosomes, plasma membranes, and the ECM, emphasizing the role of intercellular communication and membrane-associated signaling in cognitive decline. Pathway analyses further highlighted amyloid fibril formation, energy metabolism, synaptic signaling, and cellular adhesion as key processes altered in the transition from CU to CI. The convergence of electrolyte, metabolite, lipid, and protein changes highlights early multisystem dysregulation involving neuronal excitability, synaptic integrity, mitochondrial function, membrane composition, and ECM remodeling (**Table 4, and Fig. 8**). Importantly, several of the molecules identified,including potassium, DTBHQ, N-amidino-aspartic acid, lauroylcarnitine, and multiple ECM proteins, represent previously unreported CSF biomarkers, highlighting the novelty of our multiomics approach.

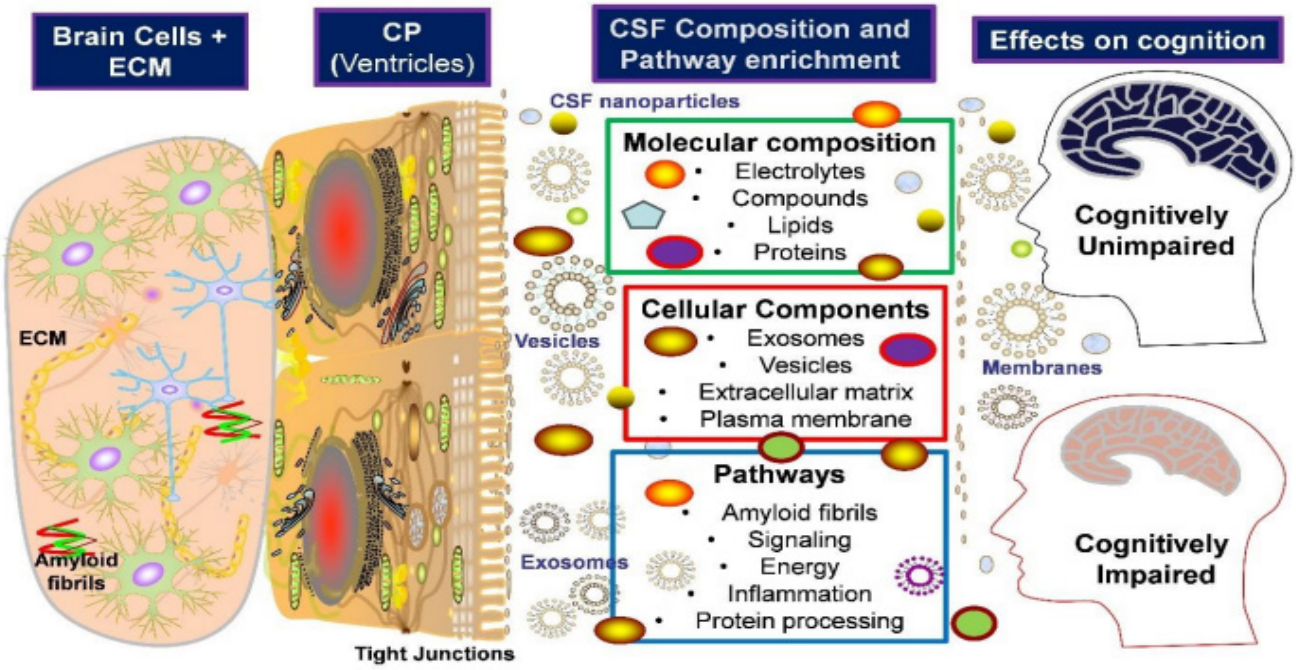
Table 3. List of protein classes that were significantly altered in the CSF from CI participants (P value < 0.05).

Proteins	Protein Classification/Function
Lumican, matrilin-2, chondroadherin, thrombospondin-4, collagen alpha-1(XVIII) chain	Extracellular matrix proteins
Amyloid-beta precursor protein, desmoglein-2, protocadherin-17, VPS10 domain-containing receptor SorCS3, transforming growth factor beta receptor type 3, glycoprotein NMB, vasorin, neuroligin-1, cell adhesion molecule 3, neural cell adhesion molecule 2, LINGO3, sodium channel subunit β-2, zinc transporter ZIP10, cell adhesion molecule 1, vesicular integral-membrane protein VIP36, transmembrane emp24 domain-containing protein 4, reticulon-4 receptor-like 2, N-acetyllactosaminide beta-1,3-N-acetylglucosaminyltransferase 2, protein ERGIC-53, epidermal growth factor receptor, beta-galactoside alpha-2,6-sialyltransferase 2, VPS10 domain-containing receptor SorCS2, ER membrane protein complex subunit 10, phosphoinositide-3-kinase-interacting protein 1, protein disulfide-isomerase	Transmembrane proteins
Tyrosine-protein phosphatase non-receptor type substrate 1, protein ABHD14B, microtubule-associated protein, heat shock 70 kDa protein 1A, SH3 domain-binding glutamic acid-rich-like protein, cellular retinoic acid-binding protein 1, myosin-2, next to BRCA1 gene 1 protein, serine/threonine-protein phosphatase 5, eukaryotic translation initiation factor 4 gamma 3, creatine kinase M-type, thioredoxin, alpha-enolase, peptidyl-prolyl cis-trans isomerase FKBP1A	Cytoplasmic proteins
Ephrin-A1, beta-2-microglobulin	Cell surface proteins
Voltage-dependent calcium channel subunit alpha-2/delta-2, monocyte differentiation antigen CD14, ciliary neurotrophic factor receptor subunit alpha	Glycosylphosphatidylinositol (GPI)-anchored proteins
Noelin, neuroserpin, semaphorin-3G, neurexophilin-4, ribonuclease T2, insulin-like growth factor-binding protein 3,ceruloplasmin	Secreted proteins
Glyoxalase domain-containing protein 4	Mitochondrial protein
Pro-cathepsin H, alpha-N-acetylgalactosaminidase	Lysosomal protein
Reticulocalbin-2	Calcium-binding protein
Chymotrypsinogen A	Zymogen
Polypeptide N-acetylgalactosaminyltransferase 16	Glycosyltransferase protein
Gelsolin	Actin-binding protein
Coagulation factor XIII B chain, coagulation factor XI, complement C2, hemopexin	Glycoproteins
Non-secretory ribonuclease	RNA-binding protein
Ribonuclease inhibitor	Leucine-rich repeat (LRR) protein
Actin, alpha skeletal muscle	Contractile protein

Table 4. Major mechanisms that are related to cognitive impairment and the metabolites associated with it.

Mechanisms	Metabolites
Energy	DTBHQ, lauroylcarnitine, creatine, reticulocalbin-2, myristic acid, acylcarnitines
Inflammation	Kynurenine, erucamide, phosphoinositides, sphingolipids, myristic acid
Signaling	Potassium, myristic acid, ornithine, N-amidino-aspartic acid, phosphoinositides, docosanamide, lauroylcarnitine, oleamide, phosphatidylcholine, cholesterol, sphingolipids, ephrin-A1, chondroadherin, reticulocalbin-2
Protein processing	Phosphatidylinositol-3-phosphate, cholesterol, amyloid precursor protein, polypeptide N-acetylgalactosaminyltransferase 16
Membrane remodeling/growth	Cholesterol, chondroadherin
Neurotransmitter function	Oleamide, erucamide
Cytosis	Phosphoinositides
Cell growth	Sphingolipids, cholesterol
Others (oxidation, aging, sleep, gut-brain axis)	DTBHQ, erucamide, oleamide, myristic acid

Figure 8. Summary schema of major cerebrospinal fluid (CSF) molecular changes associated with cognitive impairment. Electrolytes, compounds, lipids, and proteins were detected in the CSF of older adults at the cognitively unimpaired (CU) and cognitively impaired (CI) stages during follow-up via a multiomics approach. Analysis of cellular components revealed that CSF proteins were enriched in exosomes, vesicles, the extracellular matrix, and the plasma membrane. Biological pathway analysis revealed alterations in amyloid fibril formation, signaling, inflammatory processes, protein processing, and energy metabolism pathways in participants who developed cognitive impairment.



Translational implications

The identification of these novel molecules provides a foundation for early biomarker development and mechanistic research on cognitive decline. By capturing molecular alterations that precede clinical symptoms, these findings may inform early intervention strategies targeting energy metabolism, synaptic signaling, lipid homeostasis, and ECM integrity. Moreover, the integration of electrolytes, metabolites, lipids, and proteins underscores the value of multiomics approaches in elucidating complex, interconnected pathways that contribute to neurodegeneration.

Strengths and Limitations

A major strength of this study is its longitudinal design, in which each participant was profiled in both the cognitively unimpaired and impaired states. By using individuals as their own controls, we substantially reduce genetic, environmental, and lifestyle heterogeneity, enabling the detection of subtle yet biologically meaningful molecular changes that might otherwise be obscured in larger cross-sectional studies. Several limitations should be acknowledged. Since no longitudinal control group of cognitively unimpaired non-converters was included, age-related changes cannot be distinguished from cognitive decline-specific changes. Amyloid and tau biomarkers were not used to define participant status, precluding disease-specific conclusions regarding Alzheimer's pathology. Although the sample size was modest (n=8), this design however provides unusually high-resolution insight into early disease-associated processes. Importantly, our results illustrate how deep molecular phenotyping in small, carefully followed cohorts can reveal candidate biomarkers and pathways that merit validation in larger populations. The findings should therefore be interpreted as hypothesis-generating for larger confirmatory studies. This approach also sets the stage for precision medicine strategies, where longitudinal molecular profiling could identify individuals at risk and inform targeted interventions before irreversible cognitive decline occurs.

CONCLUSION

Collectively, our findings provide a hypothesis-generating view of molecular changes associated with the transition from cognitively unimpaired to cognitively impaired states (Fig. 8). This study highlights candidate CSF molecules and pathways that warrant validation in larger, independent cohorts across multiple biochemical classes (**Table 5**) and highlights mechanistic pathways that may be pivotal in the transition from CU to CI. These results provide a compelling rationale for further validation in larger cohorts and offer promising leads for early diagnostic and therapeutic strategies in Alzheimer's disease and related dementias.

Table 5. List of novel CSF molecules associated with early cognitive impairment/AD from our dataset

Molecule Class	Molecule	Change in CI vs CU	Potential Mechanistic Insight	Novelty in AD Research
Electrolyte	Potassium (K+)	↓	Maintains neuronal excitability and synaptic transmission; decreased levels may impair cognitive signaling	Rarely reported in CSF of CI or AD patients
Compound	2,5-di-tert-butylhydroquinone (DTBHQ)	↓	Antioxidant, protects mitochondria, supports neuronal energy metabolism	Novel in AD CSF studies
Compound	Creatine	↓	Brain energy homeostasis, ATP regeneration, mitochondrial support	Limited CSF evidence in early cognitive decline
Compound	Ornithine	↑	Urea cycle metabolism, polyamine synthesis; excess may disrupt neurotransmission	Not commonly reported in CSF AD studies
Compound	N-Amidino-Aspartic Acid	↑	Modulates NMDARs, synaptic plasticity, and neurodevelopment	Novel in CI/AD context
Compound	Kynurenine	↑	Tryptophan metabolism; linked to neuroactive metabolite imbalance and excitotoxicity	Increasingly studied in AD, but still limited as CSF biomarker
Fatty Acyl	Myristic acid	↓	Membrane composition, GABAergic signaling; may influence neuronal aging	Limited prior AD CSF reports
Fatty Acyl	Docosanamide	↓	Neuroprotection via energy metabolism and signaling modulation	Novel in AD CSF studies
Fatty Acyl	Oleamide	↓	Endocannabinoid signaling, microglial modulation, sleep regulation	Rarely reported in human AD CSF
Fatty Acyl	Erucamide	↓	Modulates cholinergic function, memory, angiogenesis	Not previously reported in CSF of CI/AD
Acylcarnitine	Lauroylcarnitine	↑	Mitochondrial fatty acid transport, neuroprotection	Novel in CSF of early CI
Glycerolipid	Diacylglycerol s (DG 34:1, DG 34:2, DG 36:2)	↑	Second messengers, PKC signaling, synaptic function	Rarely reported in early cognitive decline
Glycerophospholipid	PE / LysoPE	↓	Membrane integrity, neurotransmission	Potential early biomarker, limited prior CSF studies
Glycerophospholipid	Plasmenyl-PC / Plasmenyl-PE	↑	Membrane fluidity, antioxidant defense, Aβ plaque modulation	Novel CSF biomarker candidate
Sphingolipid	SM d35:2, SM d44:4, SM d43:3	↑	Membrane microdomains, cell signaling	Limited CSF evidence in AD
Sterol	Testosterone	↓	Neuroprotection, synaptic signaling	Rarely measured in early CI CSF
ECM / Cell-Matrix Protein	Lumican (P51884)	↑	ECM remodeling, synaptic plasticity	Novel in CSF AD research
ECM / Cell-Matrix Protein	Matrilin-2 (O00339)	↑	ECM organization, neuronal connectivity	Novel CSF biomarker
ECM / Cell-Matrix Protein	Desmoglein-2 (Q14126)	↑	Cell adhesion, synaptic integrity	Novel CSF biomarker
ECM / Cell-Matrix Protein	Protocadherin-17 (O14917)	↑	Synaptic adhesion and signaling	Novel CSF biomarker
ECM / Cell-Matrix Protein	Noelin (Q99784)	↑	Neuronal development, synapse formation	Limited prior studies
Cell Surface / Signaling Protein	Vasorin	↑	Modulates TGF-β signaling; vascular and neuronal effects	Novel in AD CSF

Cell Surface / Signaling Protein	SorCS3 (Q9UPU3)	↑	Receptor trafficking, neuronal sorting	Rarely reported in CSF AD research
Cell Surface / Signaling Protein	Thrombospon din-4	↑	Synaptogenesis, neurovascular signaling	Limited prior evidence
Cell Surface / Signaling Protein	Ephrin-A1 (P20827)	↓	Cell-cell communication, BBB function	CSF level changes are novel
Calcium-binding / ER Protein	Reticulocalbin-2 (Q14257)	↓	Calcium homeostasis, ER function	Novel CSF marker for cognitive impairment
ECM / Cell Adhesion Protein	Chondroadher in (O15335)	↓	Synaptic organization, perineuronal net formation	Novel in AD CSF

Supplementary Figure 1. LC-MSn quality control data suggests high measurement precision of the detected metabolites with good relative quantification, consistency, and agreement across samples and pooled quality controls. Details are outlined in the next page.

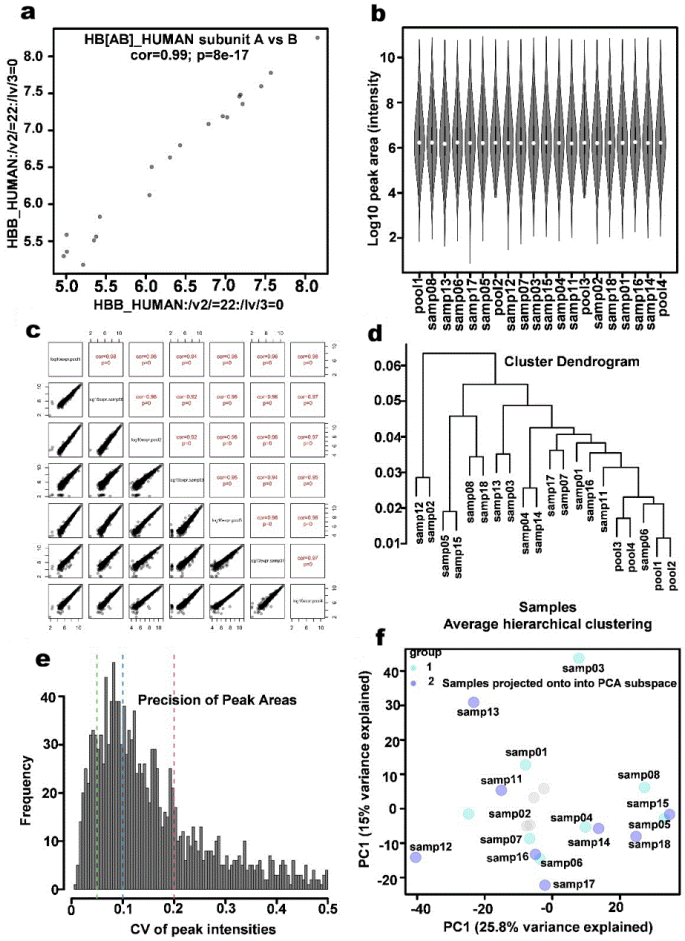


Fig. 1a: Correlation between HBB_HUMAN Subunits A vs B. This scatter plot demonstrates the strong correlation between expression levels of HBB_HUMAN subunit A (x-axis) and subunit B (y-axis). Both axes show log-transformed intensity values. The plot indicates a highly significant positive correlation between these protein subunits, suggesting good relative quantification.
Fig. 1b: The distribution of peak areas (intensity) across samples and pooled quality controls. The violin plot displays the distribution of log10-transformed peak areas (intensity) across multiple samples and pooled quality controls after average centering normalization. The y-axis represents log10 peak area intensity (ranging from ~2 to 10), while the x-axis shows different samples labeled as "pool" (quality control pools 1-4) and individual randomized samples. White dots within each violin represent median values, consistently around 6 across all samples. The similar shape and median values across samples indicate good consistency in the LC-MS analysis.
Fig. 1c: Correlation matrix of log10 peak areas (TIC) between Samples. This correlation matrix presents pairwise comparisons between different samples (pools and individual samples) based on their log10-transformed intensities. The diagonal shows sample labels, while the upper triangle displays correlation coefficients (cor) and p-values (p=0) in red. The lower triangle

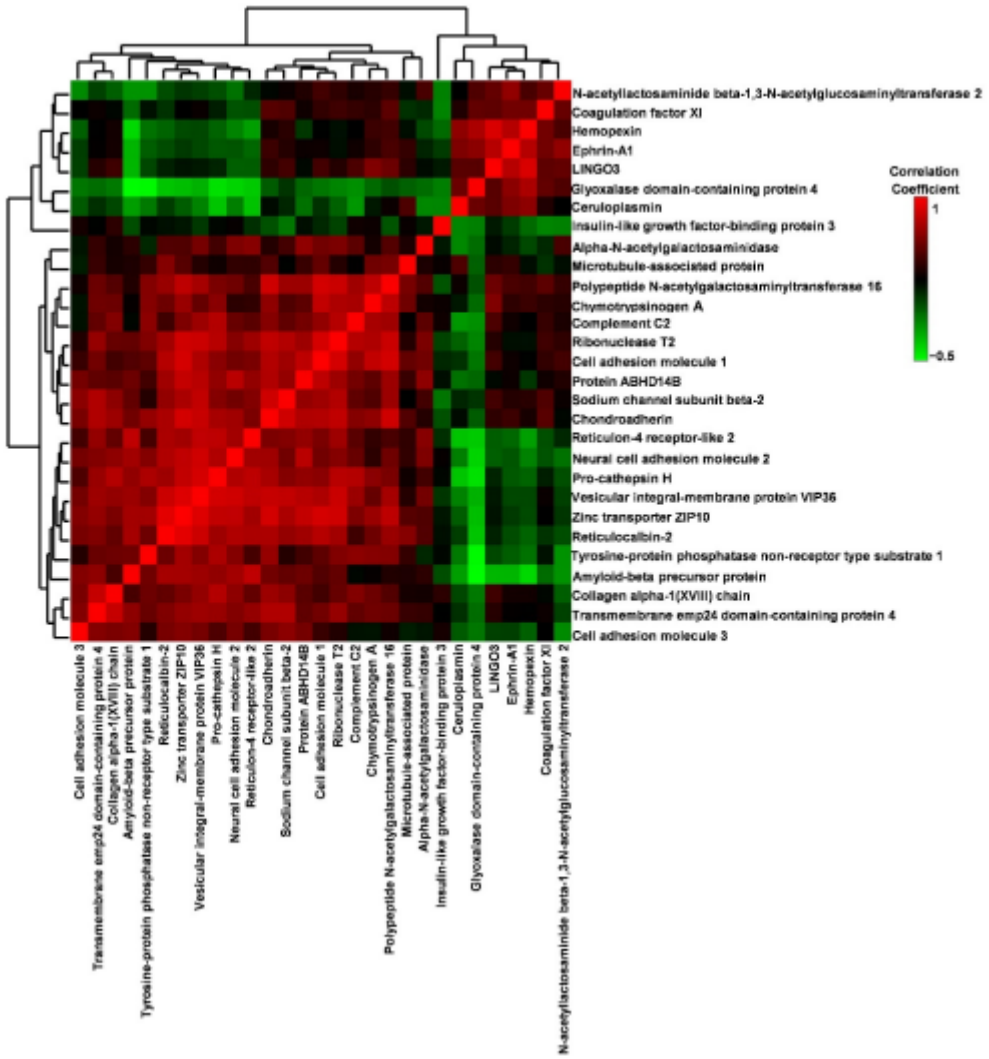
shows scatter plots of the corresponding sample pairs. All correlations are very high, demonstrating excellent agreement across both technical replicates (pools) and biological samples.

Fig. 1d: Hierarchical clustering dendrogram of pooled quality controls and CSF samples. The hierarchical clustering dendrogram illustrates the relationship between samples based on correlation distances. The y-axis represents correlation-based distance (1 - correlation coefficient), ranging from 0.01 to 0.06, with smaller values indicating higher similarity. Samples are organized along the x-axis, with both individual samples (e.g.,samp01-samp18) and quality control pools (pool1-pool4) displayed. Notably technical replicates from pool1 to pool4 show the closest relationship.

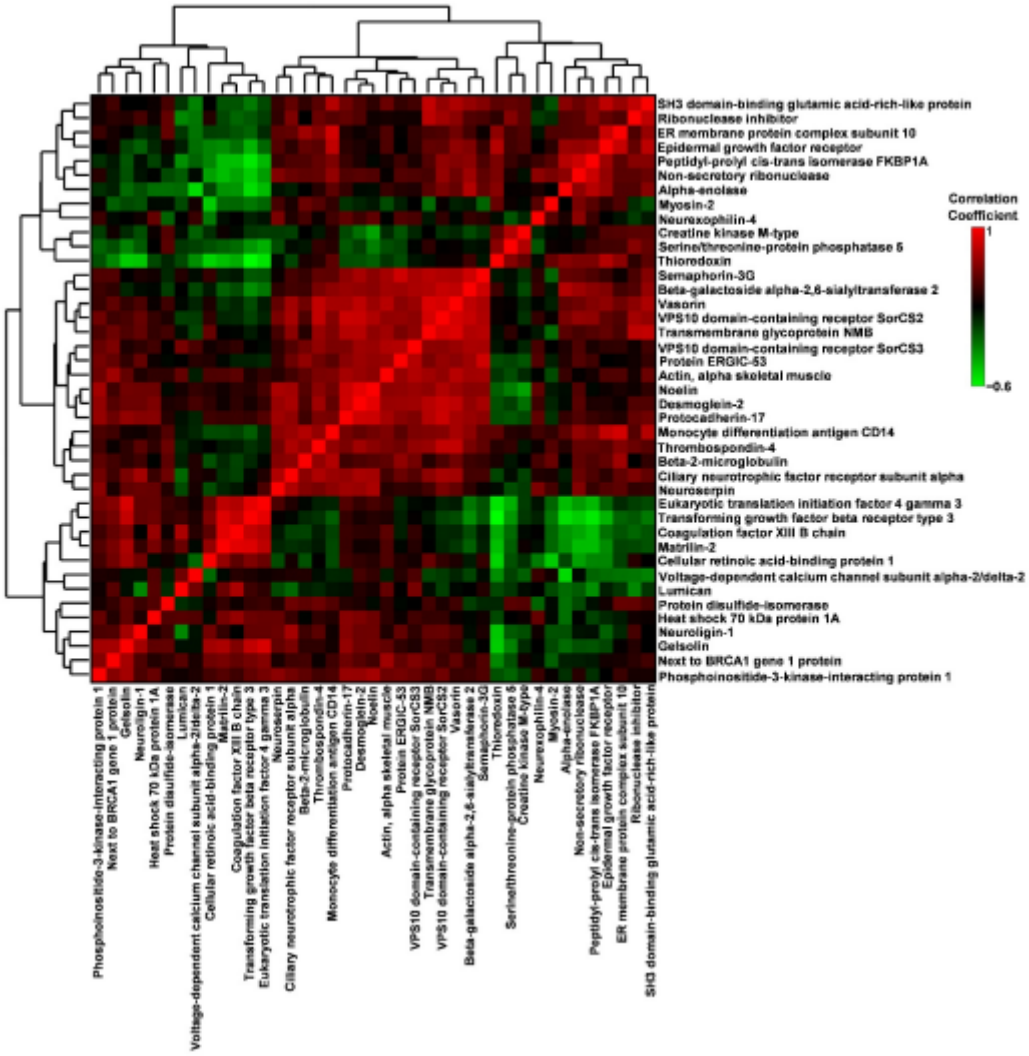
Fig. 1e: The histogram shows the distribution of coefficient of variation (CV) values for molecule intensities in the LC-MS analysis. The x-axis represents CV values ranging from 0.0 to 0.5, while the y-axis shows frequency. Three vertical dashed lines (green, blue, and red) mark key CV thresholds at 0.05, 0.1, and 0.2.Most peak areas demonstrate CVs below 0.2, with the highest frequency of peaks showing CVs between 0.05-0.1, indicating good measurement precision for most detected analytes.

Fig. 1f: Principal Component Analysis (PCA) of sample distributions. This PCA plot visualizes sample relationships in a reduced dimensionality space defined by the first two principal components. PC1 (x-axis) explains 25.8% of the total variance, while PC2 (y-axis) explains 15.8%. Samples are colored by group assignment (group 1: turquoise, group 2: blue, QC pools: grey) and labeled individually. Notable observations include: (1) substantial spread of samples along both PC axes, indicating biological heterogeneity, (2) qualitative shift but incomplete separation between groups 1 and 2, and (3) several outlier samples (samp03, samp13) showing distinct multi-omic profiles. The limited variance explained by the first two PCs suggests complex, multidimensional variation in the dataset that cannot be fully captured in the first two PCs.

Supplementary Figure 2. Correlation of CSF proteins whose levels were lower in the cognitively impaired (CI) compared to the cognitively unimpaired (CU) state. The heatmap shows the spearman rank correlation coefficient (Range from -0.5 to 1.0). Notably, there was a positive correlation between most of the proteins that were decreased with cognitive impairment state.



Supplementary Figure 3. Correlation of CSF proteins whose level increased in the cognitively impaired compared to the cognitively unimpaired state. The heatmap shows the spearman rank correlation coefficient (Range from -0.6 to 1.0). Most proteins that were found to be increased with CI state were positively correlated with each other.



Supplementary Table 1. Mean neuropsychological (NP) scores at cognitively unimpaired (CU) and cognitively impaired (CI) states of the participants. Multiple paired t-test showed higher Z-scores in the CU compared to the CI state for most domains, indicating participants at the CI state had declined neurocognitive function.

NP Z-scores	P value	Mean of CU	Mean of CI	Delta	SE of delta	t ratio	df
PURDUE PEGBOARD COMPLETED PINS (R)Z-SCORE	0.00927	0.4265	-0.4885	-0.915	0.2573	3.556	7
Long Delay Cued Recall Corr Z-Score	0.01057	0.5317	-0.149	-0.6808	0.1968	3.459	7
WAIS FSIQ	0.01677	122.2	113.5	-8.769	2.808	3.123	7
TRAILS B Z-SCORE	0.02255	0.341	-0.4277	-0.7688	0.2639	2.913	7
DKEFS TOWER Z-SCORE	0.02705	0.54	-0.332	-0.8719	0.3129	2.786	7
WAIS-III LN SEQUENCING Z-SCORE	0.03095	0.5289	-0.06587	-0.5948	0.2209	2.693	7
WAIS PIQ	0.03923	116.3	104.6	-11.69	4.621	2.53	7
BVMT-R DELAY Z-SCORE	0.04614	0.447	-0.6697	-1.117	0.4616	2.419	7
Trial 1-5 Total FR correct z score	0.06033	0.5292	-0.02404	-0.5533	0.2473	2.237	7
PURDUE PEGBOARD COMPLETED PINS (A)Z-SCORE	0.06647	-0.1271	-0.8929	-0.7657	0.342	2.239	6
WAIS VIQ	0.07381	123.5	118.1	-5.404	2.573	2.101	7
Short Delay Cued Recall Corr Z-Score	0.07705	0.07705	-0.25	-0.575	0.2776	2.071	7
TRAILS A Z-SCORE	0.08392	0.5701	-0.07606	-0.6462	0.3209	2.014	7

WAIS-III PICTURE COMP (PC) Z-SCORE	0.10833	0.8622	0.1882	-0.674	0.3663	1.84	7
BVMT-R Z-SCORE	0.15231	0.1145	-0.6797	-0.7942	0.4945	1.606	7
PURDUE PEGBOARD COMPLETED PINS (B)Z-SCORE	0.15607	0.05214	-0.8107	-0.8629	0.5322	1.621	6
PURDUE PEGBOARD COMPLETED PINS (L)Z-SCORE	0.17224	0.2726	-0.3688	-0.6414	0.414	1.549	6
Total Intrusions Z-Score	0.17545	-0.06539	-0.7933	-0.7279	0.4829	1.507	7
WAIS-III BLOCK DESIGN (BD) Z-SCORE	0.19043	0.6158	0.2418	-0.374	0.258	1.45	7
BNT Z-SCORE	0.19084	0.9895	0.4928	-0.4967	0.343	1.448	7
Long Delay FR Correct Z-Score	0.19183	0.3173	-0.1779	-0.4952	-0.4952	1.444	7
False Positives Z-Score	0.19253	0.06452	-0.4135	-0.478	0.3315	1.442	7
WAIS-III ARITHMETIC Z-SCORE	0.19499	0.4057	0.1051	-0.3006	0.2098	1.433	7
WAIS-III SIMILARITIES Z-SCORE	0.2016	1.579	1.208	-0.3712	0.2634	1.409	7
STROOP INTERFERENCE Z-SCORE	0.21485	0.4548	0.04712	-0.4077	0.2989	1.364	7
LANGUAGE ANIMALS Z-SCORE	0.31927	0.5999	0.1836	-0.4163	0.3884	1.072	7
WAIS-III DIGIT SPAN Z-SCORE	0.32201	0.3689	0.1941	-0.1748	0.1641	1.066	7
EXEC FUNC ANIMALS Z-SCORE	0.33402	0.5346	0.188	-0.3466	0.3341	1.037	7
WAIS-III MATRIX REASONING Z-SCORE	0.39638	1.149	0.7022	-0.447	0.4949	0.9033	7
JUDG LINE ORIENTATION Z-SCORE	0.43416	0.4247	0.1669	-0.2578	0.3108	0.8296	7
Short Delay FR Correct Z-Score	0.47112	0.3413	0.05769	-0.2837	-0.2837	0.7617	7
REY-O 3-MINTUTE DELAY Z-SCORE	0.49585	0.7493	0.2965	-0.4528	0.6304	0.7183	7
WAIS-III DIGIT SYMBOL Z-SCORE	0.51909	0.4254	0.137	-0.2884	0.4248	0.6788	7
LANGUAGE COWAT Z-SCORE	0.53872	0.3189	0.04538	-0.2736	0.4233	0.6463	7
List B FR Correct Z-Score	0.53977	0.5558	0.274	-0.2817	0.4371	0.6445	7
Recognition Hits Z-Score	0.551	-0.1943	-0.5337	-0.3393	0.5418	0.6263	7
LM II Z-SCORE	0.68936	0.7132	0.5863	-0.1268	0.3043	0.4167	7
WAIS-III INFORMATION Z-SCORE	0.7204	1.507	1.391	-0.1159	0.3109	0.3727	7
Trial 5 correct z score	0.72771	0.2337	0.3173	0.08365	0.2308	0.3625	7
EXEC FUNC COWAT Z-SCORE	0.73002	0.1827	0.04538	-0.1373	0.3822	0.3592	7
STROOP WORD READING Z-SCORE	0.89978	0.1234	0.05548	0.06788	0.5199	0.1306	7
LM I Z-SCORE	0.91741	0.5532	0.5813	0.02817	0.2621	0.1075	7
STROOP COLOR NAMING Z-SCORE	0.94611	0.5514	0.5329	0.01856	0.2649	0.0701	7

Delta- differences in the mean between CU and CI, SE delta- standard error, t-ratio-statistical significance, df- degrees of freedom

	Fold Change	log2(FC)
PURDUE PEGBOARD COMPLETED PINS (A) Z-SCORE	263	8.0389
PURDUE PEGBOARD COMPLETED PINS (R) Z-SCORE	8.3447	3.0609
BVMT-R DELAY Z-SCORE	4.3611	2.1247
BVMT-R Z-SCORE	3.1794	1.6687
Total Intrusions Z-Score	2.4856	1.3136
DKEFS TOWER Z-SCORE	2.3817	1.252
PURDUE PEGBOARD COMPLETED PINS (B) Z-SCORE	2.3507	1.2331
PURDUE PEGBOARD COMPLETED PINS (L) Z-SCORE	2.0111	1.008

Supplementary Table 2. List of analytes (electrolyte, compounds, lipids, and proteins) whose levels changed in cognitively impaired (CI) compared to cognitively unimpaired (CU). These data are the mean, standard deviation, and 95% confidence interval of metabolites in the CU and CI stages, percentage change from the cognitively impaired stage [(CI-CU)/CU*100], and corresponding p-values (Wilcoxon signed-rank test).

Metabolites	Cognitively unimpaired (CU)	Cognitively Impaired (CI)	Change from CU	P value
Electrolyte, Mean ± SD (95%CI)				
Potassium	9.85 ± 0.055 (9.80-9.89)	9.80 ± 0.05 (9.76-9.85)	-0.05	0.00007
Compounds, Mean ± SD (95%CI)				
2,5-di-tert-Butylhydroquinone	6.95 ± 0.052 (6.90-6.99)	6.89 ± 0.058 (6.85-6.94)	-0.06	0.0078
Creatine	10.41 ± 0.07 (10.34-10.47)	10.32 ± 0.08 (10.25-10.38)	-0.09	0.0390
Ornithine	7.99 ± 0.10 (7.91-8.08)	8.05 ± 0.09 (7.97-8.12)	0.06	0.0078

N-Amidino-Aspartic Acid	6.63 ± 0.12 (6.53-6.73)	6.71 ± 0.11 (6.62-6.79)	0.08	0.0234
Kynurenine	6.15 ± 0.21 (5.97-6.33)	6.21 ± 0.19 (6.05-6.37)	0.06	0.0468
Fatty acyls, Mean ± SD (95%CI)				
Myristic acid	5.71 ± 0.19 (5.55-5.87)	5.49 ± 0.16 (5.35-5.62)	-0.22	0.0078
Docosanamide	8.14 ± 0.05 (8.09-8.18)	8.03 ± 0.05 (7.99-8.07)	-0.11	0.0078
Oleamide	7.15 ± 0.06 (7.09-7.19)	7.07 ± 0.04 (7.03-7.11)	-0.08	0.0156
Erucamide	9.91 ± 0.05 (9.86-9.96)	9.83 ± 0.04 (9.79-9.87)	-0.08	0.0234
Lauroylcarnitine	6.19 ± 0.15 (6.06-6.31)	6.41 ± 0.31 (6.15-6.67)	0.22	0.0234
Glycerophospholipids, Mean ± SD (95%CI)				
PC 38:7	6.99 ± 0.18 (6.84-7.14)	6.79 ± 0.25 (6.58-7.00)	-0.20	0.0078
PE 40:7	6.60 ± 0.10 (6.52-6.69)	6.47 ± 0.15 (6.35-6.60)	-0.13	0.0078
LPE 18:2	6.81 ± 0.17 (6.66-6.96)	6.72 ± 0.16 (6.59-6.86)	-0.09	0.0156
PI 36:4	6.95 ± 0.03 (6.92-6.97)	6.91 ± 0.04 (6.88-6.95)	-0.04	0.0156
PC 39:7	5.44 ± 0.43 (5.09-5.79)	5.26 ± 0.33 (4.98-5.53)	-0.18	0.0391
PC[OH] OH-43:6	6.42 ± 0.22 (6.24-6.60)	6.30 ± 0.22 (6.12-6.49)	-0.12	0.0391
LPE 22:6	7.69 ± 0.14 (7.58-7.81)	7.59 ± 0.15 (7.46-7.72)	-0.10	0.0391
PC P-36:4	6.91 ± 0.09 (6.84-6.99)	6.98 ± 0.08 (6.92-7.05)	0.07	0.0078
LPC(0:0/18:0)	6.06 ± 0.15 (5.93-6.18)	6.24 ± 0.15 (6.11-6.36)	0.18	0.0078
PC 44:5	4.79 ± 1.01 (3.95-5.65)	5.29 ± 0.48 (4.88-5.69)	0.50	0.0078
LPC(18:0/0:0)	7.59 ± 0.12 (7.49-7.68)	7.69 ± 0.15 (7.57-7.82)	0.10	0.0156
PC O-36:4	6.87 ± 0.07 (6.82-6.93)	6.93 ± 0.07 (6.88-6.99)	0.06	0.0234
PC 46:9	5.69 ± 0.26 (5.48-5.91)	5.82 ± 0.19 (5.65-5.99)	0.13	0.0234
PC P-34:0	7.33 ± 0.05 (7.29-7.37)	7.36 ± 0.06 (7.31-7.40)	0.03	0.0390
PE P-36:4	7.07 ± 0.05 (7.03-7.11)	7.12 ± 0.09 (7.04-7.20)	0.05	0.0390
PC P-32:0	6.50 ± 0.17 (6.36-6.64)	6.59 ± 0.12 (6.49-6.69)	0.09	0.0390
PC 35:0	5.95 ± 0.07 (5.89-6.00)	6.06 ± 0.09 (5.97-6.14)	0.11	0.0390
PC P-38:4	6.88 ± 0.10 (6.79-6.97)	6.95 ± 0.08 (6.88-7.02)	0.07	0.0468
Sterol lipids, Mean ± SD (95%CI)				
Testosterone	6.75 ± 0.06 (6.69-6.80)	6.66 ± 0.08 (6.59-6.72)	-0.09	0.0234
Sphingolipids, Mean ± SD (95%CI)				
SM d36:1	7.07 ± 0.09 (6.99-7.15)	6.98 ± 0.12 (6.88-7.08)	-0.09	0.0078
SM C24:1	8.34 ± 0.08 (8.27-8.41)	8.29 ± 0.07 (8.24-8.36)	-0.05	0.0234
SHexCer d42:2	7.42 ± 0.15 (7.29-7.55)	7.32 ± 0.14 (7.21-7.44)	-0.10	0.0234
SM d41:6	5.60 ± 0.34 (5.31-5.88)	5.07 ± 1.05 (4.19-5.95)	-0.53	0.0390
SM d41:3	4.89 ± 1.76 (3.41-6.36)	4.64 ± 1.67 (3.25-6.04)	-0.25	0.0390
SM d35:2	6.33 ± 0.16 (6.19-6.46)	6.37 ± 0.17 (6.22-6.51)	0.04	0.0078
SM d44:4	6.13 ± 0.19 (5.97-6.29)	6.22 ± 0.16 (6.09-6.36)	0.09	0.0234
SM d43:3	5.81 ± 0.23 (5.62-6.00)	5.89 ± 0.22 (5.71-6.08)	0.08	0.0390
SM d(18:1/16:0)	9.08 ± 0.15 (8.96-9.21)	9.16 ± 0.16 (9.02-9.29)	0.08	0.0390
Proteins, Mean ± SD (95%CI)				
P20827	7.66 ± 0.07 (7.61-7.72)	7.51 ± 0.13 (7.39-7.61)	-0.15	0.0078
Q14257	5.86 ± 0.19 (5.69-6.02)	5.69 ± 0.26 (5.46-5.91)	-0.17	0.0078
O15335	5.49 ± 0.19 (5.34-5.66)	5.33 ± 0.17 (5.19-5.47)	-0.16	0.0078
P00766	6.19 ± 0.13 (6.08-6.29)	6.08 ± 0.16 (5.95-6.21)	-0.11	0.0078
Q8N428	7.81 ± 0.28 (7.58-8.05)	7.66 ± 0.22 (7.48-7.85)	-0.15	0.0078
P05067	6.80 ± 0.10 (6.72-6.89)	6.76 ± 0.14 (6.64-6.88)	-0.04	0.0078
Q8N126	6.28 ± 0.09 (6.20-6.35)	6.13 ± 0.12 (6.03-6.24)	-0.15	0.0156
Q9ULF5	6.26 ± 0.16 (6.12-6.39)	6.11 ± 0.21 (5.93-6.28)	-0.15	0.0156
P03951	5.70 ± 0.17 (5.56-5.85)	5.53 ± 0.21 (5.36-5.71)	-0.17	0.0156
O15394	6.54 ± 0.07 (6.48-6.60)	6.50 ± 0.09 (6.42-6.58)	-0.04	0.0156
P78324	6.85 ± 0.29 (6.61-7.09)	6.79 ± 0.34 (6.51-7.07)	-0.06	0.0156
Q96IU4	5.36 ± 0.27 (5.13-5.58)	5.08 ± 0.29 (4.84-5.33)	-0.28	0.0234
Q9BY67	6.65 ± 0.11 (6.57-6.74)	6.57 ± 0.13 (6.46-6.68)	-0.08	0.0234
Q12907	6.35 ± 0.11 (6.26-6.45)	6.28 ± 0.14 (6.17-6.40)	-0.07	0.0234

P0C6S8	6.34 ± 0.11 (6.25-6.44)	6.21 ± 0.16 (6.08-6.34)	-0.13	0.0234
P09668	6.20 ± 0.07 (6.14-6.26)	6.14 ± 0.09 (6.06-6.22)	-0.06	0.0234
P00450	6.95 ± 0.10 (6.87-7.04)	6.90 ± 0.10 (6.81-6.99)	-0.05	0.0234
Q7Z7H5	5.89 ± 0.14 (5.77-6.00)	5.71 ± 0.21 (5.62-5.80)	-0.18	0.0390
O60939	5.89 ± 0.26 (5.67-6.11)	5.63 ± 0.28 (5.39-5.86)	-0.26	0.0390
P06681	6.44 ± 0.13 (6.33-6.54)	6.35 ± 0.12 (6.24-6.45)	-0.09	0.0391
P17936	5.10 ± 0.22 (4.92-5.28)	4.91 ± 0.15 (4.79-5.04)	-0.19	0.0391
P02790	7.64 ± 0.11 (7.55-7.73)	7.58 ± 0.10 (7.49-7.66)	-0.06	0.0391
Q86UN3	5.91 ± 0.17 (5.77-6.05)	5.76 ± 0.19 (5.61-5.92)	-0.15	0.0391
A0A7P0T936	4.99 ± 0.25 (4.78-5.20)	4.63 ± 0.48 (4.23-5.04)	-0.36	0.0391
Q9NY97	6.13 ± 0.33 (5.86-6.40)	5.94 ± 0.39 (5.62-6.27)	-0.19	0.0391
Q9HC38	6.26 ± 0.14 (6.14-6.38)	6.18 ± 0.16 (6.04-6.32)	-0.08	0.0391
P39060	6.35 ± 0.06 (6.29-6.41)	6.22 ± 0.11 (6.13-6.31)	-0.13	0.0391
O00584	5.69 ± 0.18 (5.54-5.85)	5.53 ± 0.27 (5.31-5.76)	-0.16	0.0391
P17050	5.68 ± 0.13 (5.58-5.79)	5.63 ± 0.12 (5.52-5.73)	-0.05	0.0391
O00339	6.25 ± 0.19 (6.09-6.40)	6.45 ± 0.14 (6.33-6.56)	0.20	0.0078
P51884	6.68 ± 0.08 (6.61-6.75)	6.77 ± 0.09 (6.69-6.84)	0.09	0.0078
P06396	7.16 ± 0.04 (7.12-7.19)	7.21 ± 0.05 (7.17-7.25)	0.05	0.0078
Q14126	5.48 ± 0.16 (5.35-5.62)	5.62 ± 0.18 (5.46-5.77)	0.14	0.0078
O14917	5.41 ± 0.20 (5.24-5.58)	5.53 ± 0.13 (5.42-5.63)	0.12	0.0078
P05160	4.31 ± 1.05 (3.43-5.18)	4.92 ± 0.35 (4.62-5.21)	0.61	0.0078
Q03167	7.09 ± 0.14 (6.97-7.21)	7.16 ± 0.16 (7.02-7.29)	0.07	0.0078
P10153	5.65 ± 0.15 (5.52-5.78)	5.72 ± 0.16 (5.59-5.86)	0.07	0.0078
P13489	4.92 ± 0.26 (4.71-5.14)	5.12 ± 0.21 (4.95-5.29)	0.20	0.0078
Q9UPU3	5.20 ± 0.19 (5.04-5.36)	5.35 ± 0.17 (5.20-5.49)	0.15	0.0078
P61769	7.77 ± 0.06 (7.72-7.83)	7.83 ± 0.05 (7.79-7.88)	0.06	0.0156
P49257	7.61 ± 0.06 (7.56-7.66)	7.69 ± 0.07 (7.63-7.75)	0.08	0.0156
P68133	6.13 ± 0.07 (6.07-6.19)	6.22 ± 0.10 (6.13-6.32)	0.09	0.0156
P00533	5.61 ± 0.16 (5.48-5.75)	5.72 ± 0.18 (5.57-5.88)	0.11	0.0156
Q96JF0	5.96 ± 0.17 (5.82-6.10)	6.04 ± 0.14 (5.92-6.16)	0.08	0.0156
Q14956	5.91 ± 0.14 (5.79-6.03)	5.99 ± 0.16 (5.86-6.14)	0.08	0.0156
Q99574	6.58 ± 0.07 (6.52-6.64)	6.61 ± 0.06 (6.56-6.66)	0.03	0.0156
Q96PQ0	6.08 ± 0.09 (6.01-6.16)	6.19 ± 0.06 (6.14-6.24)	0.11	0.0234
Q5UCC4	5.69 ± 0.17 (5.55-5.84)	5.82 ± 0.13 (5.71-5.92)	0.13	0.0234
Q6EMK4	6.29 ± 0.08 (6.23-6.37)	6.37 ± 0.09 (6.29-6.45)	0.08	0.0234
Q9NY47	5.83 ± 0.10 (5.74-5.92)	5.90 ± 0.09 (5.83-5.98)	0.07	0.0234
Q9NS98	5.75 ± 0.07 (5.69-5.81)	5.81 ± 0.07 (5.75-5.87)	0.06	0.0234
P35443	5.06 ± 0.18 (4.90-5.21)	5.22 ± 0.13 (5.11-5.34)	0.16	0.0234
P0DMV8	4.24 ± 0.89 (3.49-4.99)	4.67 ± 1.07 (3.76-5.71)	0.43	0.0234
O75368	5.49 ± 0.15 (5.37-5.62)	5.59 ± 0.19 (5.44-5.75)	0.10	0.0234
P29762	4.80 ± 0.25 (4.59-5.01)	4.98 ± 0.32 (4.71-5.25)	0.18	0.0234
O95158	5.39 ± 0.15 (5.26-5.52)	5.48 ± 0.16 (5.34-5.61)	0.09	0.0312
Q96FE7	5.87 ± 0.28 (5.63-6.10)	6.09 ± 0.16 (5.95-6.23)	0.22	0.0390
Q8N2Q7	5.85 ± 0.13 (5.73-5.96)	5.94 ± 0.11 (5.84-6.03)	0.09	0.0390
Q9UKX2	4.89 ± 0.25 (4.68-5.10)	5.07 ± 0.23 (4.87-5.27)	0.18	0.0390
P08571	6.64 ± 0.10 (6.56-6.73)	6.73 ± 0.11 (6.63-6.82)	0.09	0.0390
Q14596	4.46 ± 0.40 (4.13-4.80)	4.84 ± 0.39 (4.51-5.17)	0.38	0.0390
P07237	4.28 ± 0.86 (3.57-5.00)	4.72 ± 0.34 (4.44-5.00)	0.44	0.0390
P26992	5.62 ± 0.15 (5.49-5.75)	5.72 ± 0.08 (5.65-5.79)	0.10	0.0390
Q99784	5.69 ± 0.23 (5.49-5.88)	5.82 ± 0.11 (5.72-5.91)	0.13	0.0390
P53041	4.55 ± 0.70 (3.97-5.14)	4.99 ± 0.65 (4.45-5.55)	0.44	0.0390
O43432	8.45 ± 0.17 (8.31-8.59)	8.51 ± 0.21 (8.34-8.68)	0.06	0.0390
P06732	5.58 ± 0.06 (5.53-5.63)	5.66 ± 0.04 (5.62-5.69)	0.08	0.0390
P10599	5.94 ± 0.13 (5.83-6.05)	5.99 ± 0.09 (5.92-6.07)	0.05	0.0390

P06733	6.14 ± 0.09 (6.06-6.22)	6.19 ± 0.13 (6.08-6.30)	0.05	0.0390
P62942	5.76 ± 0.12 (5.66-5.87)	5.85 ± 0.16 (5.71-5.98)	0.09	0.0468

Supplementary Table 3. UniProt IDs and the names of proteins whose levels change in the cognitively impaired compared to the cognitively unimpaired state.

Sl.No.	Uniport ID	Proteins
1	P20827	Ephrin-A1
2	Q14257	Reticulocalbin-2
3	O15335	Chondroadherin
4	P00766	Chymotrypsinogen A
5	Q8N428	Polypeptide N-acetylgalactosaminyltransferase 16
6	P05067	Amyloid-beta precursor protein
7	Q8N126	Cell adhesion molecule 3
8	Q9ULF5	Zinc transporter ZIP10
9	P03951	Coagulation factor XI
10	O15394	Neural cell adhesion molecule 2
11	P78324	Tyrosine-protein phosphatase non-receptor type substrate 1
12	Q96IU4	Protein ABHD14B
13	Q9BY67	Cell adhesion molecule 1
14	Q12907	Vesicular integral-membrane protein VIP36
15	P0C6S8	LINGO3
16	P09668	Pro-cathepsin H
17	P00450	Ceruloplasmin
18	Q7Z7H5	Transmembrane emp24 domain-containing protein 4
19	O60939	Sodium channel subunit beta-2
20	P06681	Complement C2
21	P17936	Insulin-like growth factor-binding protein 3
22	P02790	Hemopexin
23	Q86UN3	Reticulon-4 receptor-like 2
24	A0A7P0T936	Microtubule-associated protein
25	Q9NY97	N-acetyllactosaminide beta-1,3-N-acetylglucosaminyltransferase 2
26	Q9HC38	Glyoxalase domain-containing protein 4
27	P39060	Collagen alpha-1(XVIII) chain
28	O00584	Ribonuclease T2
29	P17050	Alpha-N-acetylgalactosaminidase
30	O00339	Matrilin-2
31	P51884	Lumican
32	P06396	Gelsolin
33	Q14126	Desmoglein-2
34	O14917	Protocadherin-17
35	P05160	Coagulation factor XIII B chain
36	Q03167	Transforming growth factor beta receptor type 3
37	P10153	Non-secretory ribonuclease
38	P13489	Ribonuclease inhibitor
39	Q9UPU3	VPS10 domain-containing receptor SorCS3
40	P61769	Beta-2-microglobulin
41	P49257	Protein ERGIC-53
42	P68133	Actin, alpha skeletal muscle
43	P00533	Epidermal growth factor receptor
44	Q96JF0	Beta-galactoside alpha-2,6-sialyltransferase 2
45	Q14956	Transmembrane glycoprotein NMB

46	Q99574	Neuroserpin
47	Q96PQ0	VPS10 domain-containing receptor SorCS2
48	Q5UCC4	ER membrane protein complex subunit 10
49	Q6EMK4	Vasorin
50	Q9NY47	Voltage-dependent calcium channel subunit alpha-2/delta-2
51	Q9NS98	Semaphorin-3G
52	P35443	Thrombospondin-4
53	P0DMV8	Heat shock 70 kDa protein 1A
54	O75368	SH3 domain-binding glutamic acid-rich-like protein
55	P29762	Cellular retinoic acid-binding protein 1
56	O95158	Neurexophilin-4
57	Q96FE7	Phosphoinositide-3-kinase-interacting protein 1
58	Q8N2Q7	Neuroligin-1
59	Q9UKX2	Myosin-2
60	P08571	Monocyte differentiation antigen CD14
61	Q14596	Next to BRCA1 gene 1 protein
62	P07237	Protein disulfide-isomerase
63	P26992	Ciliary neurotrophic factor receptor subunit alpha
64	Q99784	Noelin
65	P53041	Serine/threonine-protein phosphatase 5
66	O43432	Eukaryotic translation initiation factor 4 gamma 3
67	P06732	Creatine Kinase M-type
68	P10599	Thioredoxin
69	P06733	Alpha-enolase
70	P62942	Peptidyl-prolyl cis-trans isomerase FKBP1A

Acknowledgments

This work was supported by the L.K. Whittier Foundation at the Huntington Medical Research Institutes. A.V.'s contributions were supported by R01MH110438 from the National Institute of Mental Health.

Statement on Competing Interests

All the authors declare that they have no competing interests.

Data and Materials Availability

All other data needed to evaluate the conclusions in this paper are presented in the paper and/or the Supplementary Materials.

Author Contributions

A.V. and A.N.F. conceived and designed the project. N.A., R.B., and X.W. collected demographic and clinical data. S.K. and A.N. conducted the analysis of the neuropsychological data. Multiomics data were acquired by A.Q. and O.C. J.J. and A.N.F. analyzed the multiomics data. J.J., A.N.F, and A.V. prepared the figures and tables. J.J., A.N.F.,and A.V. wrote the manuscript. R.K., A.N.F., and A.V. supervised the research and coordinated all aspects of the project. All the authors reviewed and approved the final manuscript.

Footnote

This article is dedicated to the memory of our colleague, Alfred N. Fonteh, who passed away before submission of this manuscript.

REFERENCES

1. Bjorklund, G.; Aaseth, J.; Dadar, M.; Chirumbolo, S. Molecular Targets in Alzheimer's Disease. Mol Neurobiol 2019, 56, 7032–7044, doi:10.1007/s12035-019-1563-9.

2. Calabro, M.; Rinaldi, C.; Santoro, G.; Crisafulli, C. The biological pathways of Alzheimer disease: a review. AIMS Neurosci 2021, 8, 86–132, doi:10.3934/Neuroscience.2021005.

3. Dhapola, R.; Hota, S.S.; Sarma, P.; Bhattacharyya, A.; Medhi, B.; Reddy, D.H. Recent advances in molecular pathways and therapeutic implications targeting neuroinflammation forAlzheimer's disease.Inflammopharmacology 2021,29,1669–1681,doi:10.1007/s10787-021-00889-6.

4. Seto, M.; Weiner, R.L.; Dumitrescu, L.; Hohman, T.J. Protective genes and pathways in Alzheimer's disease: moving towards precision interventions. Mol Neurodegener 2021,16, 29, doi:10.1186/s13024-021-00452-5.

5. Bloom, G.S. Amyloid-beta and tau: the trigger and bullet in Alzheimer disease pathogenesis. JAMA Neurol 2014, 71, 505–508, doi:10.1001/jamaneurol.2013.5847.

6. Guo, T.; Zhang, D.; Zeng, Y.; Huang, T.Y.; Xu, H.; Zhao, Y. Molecular and cellular mechanisms underlying the pathogenesis of Alzheimer's disease. Mol Neurodegener 2020, 15, 40, doi:10.1186/s13024-020-00391-7.

7. Tackenberg, C.; Nitsch, R.M. The secreted APP ectodomain sAPPalpha, but not sAPPbeta, protects neurons against Abeta oligomer-induced dendritic spine loss and increased tau phosphorylation. Mol Brain 2019, 12, 27, doi:10.1186/s13041-019-0447-2.

8. DeTure, M.A.; Dickson, D.W. The neuropathological diagnosis of Alzheimer's disease. Mol Neurodegener 2019, 14, 32, doi:10.1186/s13024-019-0333-5.

9. Metaxas, A.; Kempf, S.J. Neurofibrillary tangles in Alzheimer's disease: elucidation of the molecular mechanism by immunohistochemistry and tau protein phospho-proteomics.Neural Regen Res 2016, 11, 1579–1581, doi:10.4103/1673-5374.193234.

10. Bhatt, S.; Puli, L.; Patil, C.R. Role of reactive oxygen species in the progression of Alzheimer's disease. Drug DiscovToday2021,26,794–803,doi:10.1016/j.drudis.2020.12.004.

11. Nasb, M.; Tao, W.; Chen, N. Alzheimer's Disease Puzzle: Delving into Pathogenesis Hypotheses. Aging Dis 2024, 15, 43–73, doi:10.14336/AD.2023.0608.

12. Kocahan, S.; Dogan, Z. Mechanisms of Alzheimer's Disease Pathogenesis and Prevention: The Brain, Neural Pathology, N-methyl-D-aspartate Receptors, Tau Protein and Other Risk Factors.Clin Psychopharmacol Neurosci 2017,15,1–8,doi:10.9758/cpn.2017.15.1.1.

13. Yao, Q.; Jiang, K.; Lin, F.; Zhu, T.; Khan, N.H.; Jiang, E. Pathophysiological Association of Alzheimer's Disease and Hypertension: A Clinical Concern for Elderly Population. Clin Interv Aging 2023, 18, 713–728, doi:10.2147/CIA.S400527.

14. Clark, C.; Rabl, M.; Dayon, L.; Popp, J. The promise of multi-omics approaches to discover biological alterations with clinical relevance in Alzheimer's disease. Front Aging Neurosci 2022, 14, 1065904, doi:10.3389/fnagi.2022.1065904.

15. Kong, A.T.; Leprevost, F.V.; Avtonomov, D.M.; Mellacheruvu, D.; Nesvizhskii, A.I.MSFragger: ultrafast and comprehensive peptide identification in mass spectrometry-based proteomics. Nat Methods 2017, 14, 513–520, doi:10.1038/nmeth.4256.

16. Hutchins, P.D.; Russell, J.D.; Coon, J.J. LipiDex: An Integrated Software Package for High-Confidence Lipid Identification.Cell Syst 2018,6,621–625 e625,doi:10.1016/j.cels.2018.03.011.

17. Hutchins, P.D.; Russell, J.D.; Coon, J.J. Mapping Lipid Fragmentation for Tailored Mass Spectral Libraries. J Am Soc Mass Spectrom 2019, 30, 659–668, doi:10.1007/s13361-018-02125-y.

18. Kind, T.; Liu, K.H.; Lee, D.Y.; DeFelice, B.; Meissen, J.K.; Fiehn, O. LipidBlast in silico tandem mass spectrometry database for lipid identification. Nat Methods 2013, 10, 755–758, doi:10.1038/nmeth.2551.

19. Tsugawa, H.; Ikeda, K.; Tanaka, W.; Senoo, Y.; Arita, M.; Arita, M. Comprehensive identification of sphingolipid species by in silico retention time and tandem mass spectral library. J Cheminform 2017, 9, 19, doi:10.1186/s13321-017-0205-3.

20. Cai, Z.; Li, H. An Updated Review: Androgens and Cognitive Impairment in Older Men.Front Endocrinol (Lausanne) 2020, 11, 586909, doi:10.3389/fendo.2020.586909.

21. Sabahat, S.E.; Saqib, M.; Talib, M.; Shaikh, T.G.; Khan, T.; Kailash, S.J. Bile acid modulation by gut microbiota: a bridge to understanding cognitive health. Ann Med Surg(Lond) 2024, 86, 5410–5415, doi:10.1097/MS9.0000000000002433.

22. Benarroch, E.E. Potassium channels: brief overview and implications in epilepsy.Neurology 2009, 72, 664–669, doi:10.1212/01.wnl.0000343739.72081.4e.

23. Cisternas, P.; Lindsay, C.B.; Salazar, P.; Silva-Alvarez, C.; Retamales, R.M.; Serrano, F.G.;Vio, C.P.; Inestrosa, N.C. The increased potassium intake improves cognitive performance and attenuates histopathological markers in a model of Alzheimer's disease. Biochim Biophys Acta 2015, 1852, 2630–2644, doi:10.1016/j.bbadis.2015.09.009.

24. Peng, S.; Shen, Y.; Wang, M.; Zhang, J. Serum and CSF Metabolites in Stroke-Free Patients Are Associated With Vascular Risk Factors and Cognitive Performance. Front Aging Neurosci 2020, 12, 193, doi:10.3389/fnagi.2020.00193.

25. Adhihetty, P.J.; Beal, M.F. Creatine and its potential therapeutic value for targeting cellular energy impairment in neurodegenerative diseases. Neuromolecular Med 2008, 10, 275–290, doi:10.1007/s12017-008-8053-y.

26. Smith, A.N.; Morris, J.K.; Carbuhn, A.F.; Herda, T.J.; Keller, J.E.; Sullivan, D.K.; Taylor,M.K. Creatine as a Therapeutic Target in Alzheimer's Disease. Curr Dev Nutr 2023,

7,102011, doi:10.1016/j.cdnut.2023.102011.

27. Buerger, C.; Garbade, S.F.; Dietrich Alber, F.; Waisbren, S.E.; McCarter, R.; Kolker, S.;Burgard, P.; Urea Cycle Disorders, C. Impairment of cognitive function in ornithine transcarbamylase deficiency is global rather than domain-specific and is associated with disease onset, sex, maximum ammonium, and number of hyperammonemic events. J Inherit Metab Dis 2019, 42, 243–253, doi:10.1002/jimd.12013.

28. Guerra, G.P.; Rubin, M.A.; Mello, C.F. Modulation of learning and memory by natural polyamines. Pharmacol Res 2016, 112, 99–118, doi:10.1016/j.phrs.2016.03.023.

29. Sivashanmugam, M.; J, J.; V, U.; K, N.S. Ornithine and its role in metabolic diseases: An appraisal. Biomed Pharmacother 2017, 86, 185–194, doi:10.1016/j.biopha.2016.12.024.

30. Errico, F.; Nuzzo, T.; Carella, M.; Bertolino, A.; Usiello, A. The Emerging Role of Altered d-Aspartate Metabolism in Schizophrenia: New Insights From Preclinical Models and Human Studies. Front Psychiatry 2018, 9, 559, doi:10.3389/fpsyt.2018.00559.

31. Liu, J.; Chang, L.; Song, Y.; Li, H.; Wu, Y. The Role of NMDA Receptors in Alzheimer's Disease. Front Neurosci 2019, 13, 43, doi:10.3389/fnins.2019.00043.

32. Gonzalez-Sanchez, M.; Jimenez, J.; Narvaez, A.; Antequera, D.; Llamas-Velasco, S.;Martin, A.H.; Arjona, J.A.M.; Munain, A.L.; Bisa, A.L.; Marco, M.P.; et al. Kynurenic Acid Levels are Increased in the CSF of Alzheimer's Disease Patients. Biomolecules 2020, 10,doi:10.3390/biom10040571.

33. Liang, Y.; Xie, S.; He, Y.; Xu, M.; Qiao, X.; Zhu, Y.; Wu, W. Kynurenine Pathway Metabolites as Biomarkers in Alzheimer's Disease.Dis Markers 2022,2022,9484217,doi:10.1155/2022/9484217.

34. Desale, S.E.; Chinnathambi, S. Role of dietary fatty acids in microglial polarization in Alzheimer's disease. J Neuroinflammation 2020, 17, 93, doi:10.1186/s12974-020-01742-3.

35. Fan, L.; Borenstein, A.R.; Wang, S.; Nho, K.; Zhu, X.; Wen, W.; Huang, X.; Mortimer, J.A.;Shrubsole, M.J.; Dai, Q.; et al. Associations of circulating saturated long-chain fatty acids with risk of mild cognitive impairment and Alzheimer's disease in the Alzheimer's Disease Neuroimaging Initiative (ADNI) cohort. EBioMedicine 2023,97,104818,doi:10.1016/j.ebiom.2023.104818.

36. Shang, Q.; Chen, G.; Zhang, P.; Zhao, W.; Chen, H.; Yu, D.; Yu, F.; Liu, H.; Zhang, X.; He,J.; et al. Myristic acid alleviates hippocampal aging correlated with GABAergic signaling.Front Nutr 2022, 9, 907526, doi:10.3389/fnut.2022.907526.

37. Akyol, S.; Ugur, Z.; Yilmaz, A.; Ustun, I.; Gorti, S.K.K.; Oh, K.; McGuinness, B.; Passmore,P.; Kehoe, P.G.; Maddens, M.E.; et al. Lipid Profiling of Alzheimer's Disease Brain Highlights Enrichment in Glycerol(phospho)lipid, and Sphingolipid Metabolism. Cells 2021, 10, doi:10.3390/cells10102591.

38. Yin, F. Lipid metabolism and Alzheimer's disease: clinical evidence, mechanistic link and therapeutic promise. FEBS J 2023, 290, 1420–1453, doi:10.1111/febs.16344.

39. Wood, P.L.; Medicherla, S.; Sheikh, N.; Terry, B.; Phillipps, A.; Kaye, J.A.; Quinn, J.F.;Woltjer, R.L. Targeted Lipidomics of Fontal Cortex and Plasma Diacylglycerols (DAG) in Mild Cognitive Impairment and Alzheimer's Disease: Validation of DAG Accumulation Early in the Pathophysiology of Alzheimer's Disease. J Alzheimers Dis 2015, 48, 537–546,doi:10.3233/JAD-150336.

40. Chew, H.; Solomon, V.A.; Fonteh, A.N. Involvement of Lipids in Alzheimer's Disease Pathology and Potential Therapies. Front Physiol 2020, 11, 598, doi:10.3389/fphys.2020.00598.

41. Sprenger, K.G.; Leitzke, E.E.; Melchior, J.T.; Bruce, K.D. Lipid and Lipoprotein Metabolism in Microglia: Alzheimer's Disease Mechanisms and Interventions. J Lipid Res 2025,100872, doi:10.1016/j.jlr.2025.100872.

42. Senanayake, V.; Goodenowe, D.B. Plasmalogen deficiency and neuropathology in Alzheimer's disease: Causation or coincidence? Alzheimers Dement (N Y) 2019, 5, 524–532, doi:10.1016/j.trci.2019.08.003.

43. Su, X.Q.; Wang, J.; Sinclair, A.J. Plasmalogens and Alzheimer's disease: a review. Lipids Health Dis 2019, 18, 100, doi:10.1186/s12944-019-1044-1.

44. Meletis, C.D. Alkyl-Acylglycerols and the Important Clinical Ramifications of Raising Plasmalogens in Dementia and Alzheimer's Disease. Integr Med (Encinitas) 2020, 19, 12–16.

45. Adamu, A.; Li, S.; Gao, F.; Xue, G. The role of neuroinflammation in neurodegenerative diseases: current understanding and future therapeutic targets. Front Aging Neurosci 2024, 16, 1347987, doi:10.3389/fnagi.2024.1347987.

46. Hernandez-Diaz, C.; Juarez-Oropeza, M.A.; Mascher, D.; Pavon, N.; Regla, I.; Paredes-Carbajal, M.C. Effects of Oleamide on the Vasomotor Responses in the Rat. Cannabis Cannabinoid Res 2020, 5, 42–50, doi:10.1089/can.2019.0014.

47. Hiley, C.R.; Hoi, P.M. Oleamide: a fatty acid amide signaling molecule in the cardiovascular system? Cardiovasc Drug Rev 2007, 25, 46–60, doi:10.1111/j.1527-3466.2007.00004.x.

48. Zanettini, C.; Panlilio, L.V.; Alicki, M.; Goldberg, S.R.; Haller, J.; Yasar, S. Effects of endocannabinoid system modulation on cognitive and emotional behavior. Front Behav Neurosci 2011, 5, 57, doi:10.3389/fnbeh.2011.00057.

49. Guan, X.; Cravatt, B.F.; Ehring, G.R.; Hall, J.E.; Boger, D.L.; Lerner, R.A.; Gilula, N.B. The sleep-inducing lipid oleamide deconvolutes gap junction communication and calcium wave transmission in glial cells. J Cell Biol 1997, 139, 1785–1792,doi:10.1083/jcb.139.7.1785.

50. Mendelson, W.B.; Basile, A.S. The hypnotic actions of the fatty acid amide, oleamide.Neuropsychopharmacology 2001, 25, S36–39, doi:10.1016/S0893-133X(01)00341-4.

51. Qian, L.; Zheng, T.; Zhao, B.; Wang, W.; Wu, Y. Neonatal supplementation of oleamide during suckling ameliorates maternal postpartum sleep interruption-induced neural impairment and endocannabinoid dysfunction in early adolescent offspring rats. Front Nutr 2025, 12, 1566182, doi:10.3389/fnut.2025.1566182.

52. Yang, J.Y.; Wu, C.F.; Wang, F.; Song, H.R.; Pan, W.J.; Wang, Y.L. The serotonergic system may be involved in the sleep-inducing action of oleamide in rats. Naunyn Schmiedebergs Arch Pharmacol 2003, 368, 457–462, doi:10.1007/s00210-003-0843-z.

53. Kalaria, R.N.; Harik, S.I. Carnitine acetyltransferase activity in the human brain and its microvessels is decreased in Alzheimer's disease. Ann Neurol 1992, 32, 583–586, doi:10.1002/ana.410320417.

54. Kepka, A.; Ochocinska, A.; Borzym-Kluczyk, M.; Skorupa, E.; Stasiewicz-Jarocka, B.;Chojnowska, S.; Waszkiewicz, N. Preventive Role of L-Carnitine and Balanced Diet in Alzheimer's Disease. Nutrients 2020, 12, doi:10.3390/nu12071987.

55. Pennisi, M.; Lanza, G.; Cantone, M.; D'Amico, E.; Fisicaro, F.; Puglisi, V.; Vinciguerra, L.;Bella, R.; Vicari, E.; Malaguarnera, G. Acetyl-L-Carnitine in Dementia and Other Cognitive Disorders: A Critical Update. Nutrients 2020, 12, doi:10.3390/nu12051389.

56. Virmani, A.; Binienda, Z. Role of carnitine esters in brain neuropathology. Mol Aspects Med 2004, 25, 533–549, doi:10.1016/j.mam.2004.06.003.

57. Buhl, E.; Kim, Y.A.; Parsons, T.; Zhu, B.; Santa-Maria, I.; Lefort, R.; Hodge, J.J.L. Effects of Eph/ephrin signalling and human Alzheimer's disease-associated EphA1 on Drosophila behaviour and neurophysiology.Neurobiol Dis 2022,170,105752,doi:10.1016/j.nbd.2022.105752.

58. Hendrickson, A.S.; Francis, K.L.; Kumar, A.; Le, J.P.; Scarlett, J.M.; Keene, C.D.; Tovar,D.A.; Alonge, K.M. Assessing translational applicability of perineuronal net dysfunction in Alzheimer's disease across species. Front Neurosci 2024, 18, 1396101,doi:10.3389/fnins.2024.1396101.

59. Sun, Y.; Xu, S.; Jiang, M.; Liu, X.; Yang, L.; Bai, Z.; Yang, Q. Role of the Extracellular Matrix in Alzheimer's Disease.Front Aging Neurosci 2021, 13, 707466, doi:10.3389/fnagi.2021.707466.

60. O'Brien, R.J.; Wong, P.C. Amyloid precursor protein processing and Alzheimer's disease. Annu Rev Neurosci 2011, 34, 185–204, doi:10.1146/annurev-neuro-061010-113613.

61. Chiurchiu, V.; Maccarrone, M.; Orlacchio, A. The role of reticulons in neurodegenerative 815 diseases. Neuromolecular Med 2014, 16, 3–15, doi:10.1007/s12017-013-8271-9.